AGU100 ADVANCING EARTH AND SPACE SCIENCE

JGR Oceans

RESEARCH ARTICLE
10.1029/2019JC015144

Cross-Isobath Freshwater Exchange Within the North Atlantic Subpolar Gyre

Clark Pennelly[1], Xianmin Hu[1,2], and Paul G. Myers[1]

[1]Department of Earth and Atmospheric Sciences, University of Alberta, Edmonton, Alberta, Canada, [2]Bedford Institute of Oceanography, Fisheries and Oceans Canada, Dartmouth, Nova Scotia, Canada

Key Points:

- An increase of the freshwater transport within the West Greenland Current will result in an increase in offshore freshwater transport
- The transport of turbulent freshwater from all regions around the Labrador Sea acts to freshen the interior basin
- Salty Irminger and Labrador Sea Water typically flow onshore, removing salt from the interior basin

Correspondence to:
C. Pennelly,
pennelly@ualberta.ca

Citation:
Pennelly, C., Hu, X., & Myers, P. G. (2019). Cross-isobath freshwater exchange within the North Atlantic subpolar gyre. *Journal of Geophysical Research: Oceans*, *124*, 6831–6853. https://doi.org/10.1029/2019JC015144

Received 15 MAR 2019
Accepted 29 AUG 2019
Accepted article online 30 AUG 2019
Published online 14 OCT 2019

Abstract The amount of cross-isobath freshwater exchange within the North Atlantic subpolar gyre is estimated from numerical modelling simulations. A regional configuration of the Nucleus for European Modelling of the Ocean model is used to carry out three simulations with horizontal resolutions of 1/4°, 1/12°, and 1/4° with a 1/12° nested domain. Freshwater transport is calculated across five isobaths in six regions for three distinct water masses. Fresh Polar Water is only transported offshore from the western coast of Greenland and the southern coast of Labrador; other regions have onshore transport of freshwater or little offshore transport. The salty water masses of Irminger and Labrador Sea Water typically have onshore transport, acting to promote subsurface freshening of the Labrador Sea. The freshwater transport via the Polar Water mass experiences a large degree of seasonal variability, while the Irminger and Labrador Sea Water masses do not. Decomposing the freshwater transport into the mean and turbulent components indicates that most regions and water masses have stronger freshwater transport associated with the mean flow while the turbulent flow in often the opposite direction. The only water mass and region where the mean and turbulent freshwater transport act in the same direction is Polar Water along the western margin of Greenland. Model resolution plays an important role in determining cross-isobath exchange as our results from an identically forced simulation at 1/4° has reduced seasonal cycles, reduced transport, and sometimes transport in the opposite direction when compared against the 1/12° resolution simulations.

Plain Language Summary The Labrador Sea, between Greenland and Canada, is a region where deep water is formed, a crucial component in the oceanic transport of heat between the equator and the poles. An input of freshwater can interrupt this process by making deep water more difficult to produce. While we know the Labrador Sea receives freshwater from the surrounding currents, we are not confident where, and how much, freshwater leaves the boundary of the Labrador Sea to enter the interior region. We explore this using numerical simulations in a region where real data collection is difficult due to extreme ocean conditions. Our simulations suggest that the west coast of Greenland is the region where most of the freshwater leaves the boundary current and enters the deeper basin. The other regions either have freshwater transported toward the coast or very little transport to begin with. We also investigated the short-lived turbulent transport of freshwater which was generally flowing from the coastal region to the deep basin, often acting opposite the long-term flow.

1. Introduction

The Labrador Sea, located between Greenland and the northeastern coast of Canada, is surrounded by boundary currents carrying significant volumes of freshwater. However, the regions where freshwater leaves the boundary current and enters the interior of the Labrador Sea, impacting deep convection within, is not well understood. Fram Strait, between Svalbard and Greenland, serves as a gateway for a significant amount of fresh Arctic water which is transported southward (de Steur et al., 2018). This East Greenland Current carries around 2 Sv (1 Sv = 10^6 m^3/s) of cold and fresh Arctic water (Sutherland & Pickart, 2008; Tsubouchi et al., 2012) along the southern tip of Greenland (Figure 1d) and between 59 and 96 mSv of freshwater relative to a salinity of 34.8 (de Steur et al., 2009; Sutherland & Pickart, 2008). As the East Greenland Current flows westward past Cape Farewell it merges with a warm and salty current carrying Irminger Water (Cuny et al., 2002; de Jong et al., 2016; Lazier et al., 2002; Myers et al., 2009), with a freshwater transport between −8 and −10 mSv (referenced to 35.0, Myers et al., 2007). This current system becomes the West Greenland Current with cold and fresh water of Arctic origin at the surface as well as warm and salty Irminger Water beneath (Fratantoni and Pickart, 2007). Meltwater from Greenland supplies additional freshwater to the current

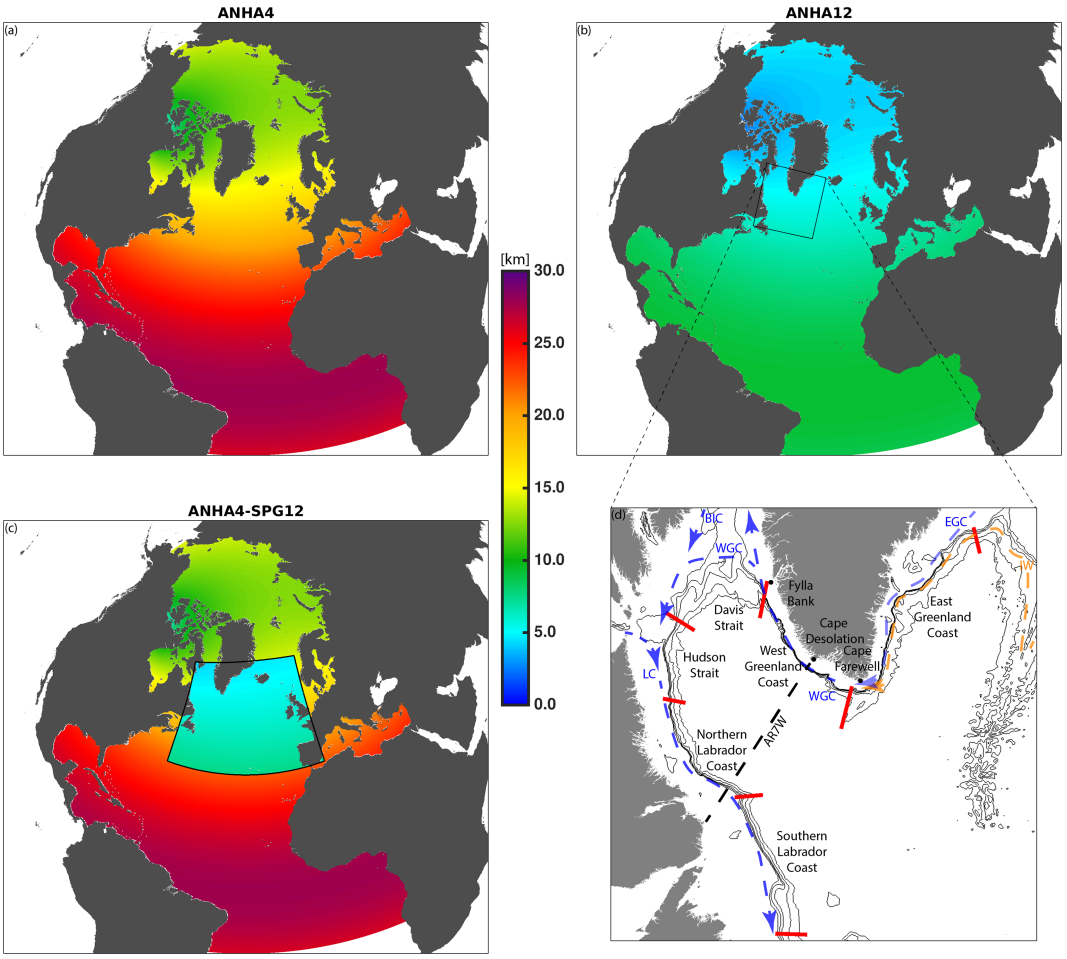

Figure 1. Domain setup for simulation ANHA4 (a), ANHA12 (b), and ANHA4 with a 1/12° nest within the subpolar gyre (SPG12) (c), with colored contours representing horizontal grid resolution. The box in (b) contains the North Atlantic subpolar gyre region (d), showing bathymetry contours for 500-, 750-, 1,000-, 1,500-, and 2,000-m depths. Red lines indicate the start and end sections of the regions analyzed in this manuscript. Surface and subsurface currents are show in (d), where abbreviations are as follows: EGC = East Greenland Current; WGC = West Greenland Current; BIC = Baffin Island Current; LC = Labrador Current; IW = Irminger Water. ANHA = Arctic Northern Hemisphere Atlantic.

system (Luo et al., 2016; Myers et al., 2009), further increasing the East and West Greenland Current's freshwater transport. After flowing north along the western coast of Greenland, the West Greenland Current splits with one path through Davis Strait into Baffin Bay (Curry et al., 2014) and the remaining path westward along the northern extent of the Labrador Sea. Outflow from Baffin Bay carries cold and fresh Arctic and Canadian Arctic water through Davis Strait with a freshwater transport between 92 and 116 mSv relative to 34.8 (Cuny et al., 2005; Curry et al., 2011; Curry et al., 2014). Hudson Strait also releases a significant amount of freshwater to the Labrador Sea, with a net freshwater transport around 38 mSv relative to 34.8 (Straneo & Saucier, 2008b). Both outflows join with the West Greenland Current, merging to become the Labrador Current (Lazier & Wright, 1993), and promote freshening of the northern Labrador Shelf (Straneo & Saucier, 2008a). The Labrador Current flows southward along the Labrador coast, past Flemish Cap, carrying a significant volume of freshwater out of the Labrador Sea.

While the above currents flow cyclonically around the Labrador Sea, regions around the Labrador Sea experience freshwater exchange between the boundary current and the interior. The western coast of Greenland has been well documented, though this is not the case for other regions around the Labrador Sea. At the southwestern tip of Greenland, offshore freshwater transport begins downstream of Cape Farwell (Lin et al., 2018). As the West Greenland Current continues northward toward Davis Strait, a

significant amount of offshore freshwater exchange occurs, upward of 60–80 mSv (Myers et al., 2009; Schmidt & Send, 2007). Ekman transport along this coast is strengthened during the winter and spring, due to northwesterly winds, amplifying offshore freshwater transport (Schulze & Frajka-Williams, 2018). Unique eddies, known as Irminger Rings, spawn within this region where topographic changes promote instability within the current system (Chanut et al., 2008; de Jong et al., 2016). These eddies are steered offshore from the current system, impacting the interior of the Labrador Sea by transporting both freshwater and heat (Kawasaki & Hasumi, 2014).

Regions downstream of the western coast of Greenland also play an important role in the freshwater exchange between the boundary currents and the Labrador Sea. From a 1/3° numerical simulation, Myers (2005) found that Arctic water flowing within the East and West Greenland Current enters the interior of the Labrador Sea in much larger quantities than the Arctic water which flows southward through Davis Strait. When Myers (2005) increased freshwater transport through Davis Strait, relatively little additional freshwater entered the interior of the Labrador Sea, suggesting that freshwater along the western rim of the Labrador Sea does not penetrate into the interior easily. Schmidt and Send (2007) suggest that the Labrador Current could supply a significant amount of freshwater toward the interior Labrador Sea. While McGeehan and Maslowski (2011) used a higher-resolution 1/12° numerical model to suggest that the Labrador Current transports freshwater offshore, they found the transport was small but not insignificant. Lagrangian particle analysis from the output of a 1/12° model simulation further support both notions that freshwater does leave the Labrador Current to enter the Labrador Sea, although in relatively low amounts (Schulze & Frajka-Williams, 2018). Many other regions around the Labrador Sea remain relatively unexplored in terms of cross-shelf freshwater exchange.

Freshwater acts to stabilize the water column by increasing stratification, thereby limiting vertical movement. However, several regions around the world have conditions that support deep convection, a process which is strongly dependent on the stratification of the water column. These regions include the Weddell and Ross Sea off Antarctica (Gordon et al., 2007; Whiteworth & Orsi, 2006), the Mediterranean Sea (Brossier et al., 2017; Marshall & Schott, 1999), the Nordic Seas (Hansen & Østerhus, 2000), the Irminger Sea (Bacon et al., 2003), and the Labrador Sea (e.g., Lab Sea Group, 1998; Lazier et al., 2002; Straneo, 2006; Yashayaev, 2007; Yashayaev & Loder, 2009; Yashayaev & Loder, 2017). Deep convection in these regions arise from certain characteristics: weak stratification, cyclonic circulation, and strong surface buoyancy loss (Marshall & Schott, 1999). Weak stratification is promoted by both the doming of the isopycnals governed by cyclonic gyre circulation (Yashayaev, 2007) and the local properties of the water masses present (Gelderloos et al., 2012). Stratification strength also depends on the history of convection, as consecutive winters with strong convection promote weak stratification, while the opposite occurs during prolonged periods with weak or no deep convection (Lab Sea Group, 1998; Lazier et al., 2002; Yashayaev, 2007; Yashayaev & Loder, 2017). While both gyre circulation (Häkkinen & Rhines, 2004) and atmospheric forcing (Yashayaev, 2007) can vary from year to year, the primary result is the homogenization of the water column, creating a deep mixed layer exceeding 1,000 m of depth in some regions. The result of this deep vertical mixing brings deep water toward the surface and modifies temperature and salinity properties throughout the mixed water column (Kieke et al., 2006; Lazier et al., 2002; Straneo, 2006; Yashayaev & Loder, 2009). Once convection ceases, the mixed layer returns close to the surface and a water mass having nearly identical properties is left behind, capped by the pycnocline.

The Labrador Sea convective season ends during spring, giving way to the restratification period. Rapid post-convection restratification occurs the first few months (Lilly et al., 1999) due to high lateral density gradients induced by convection (Frajka-Williams et al., 2014). A slower restratification process occurs afterward, causing the interior properties to shift over time toward the property profile of the surrounding boundary currents (Lilly et al., 1999; Straneo, 2006). This was evident during a period when convection was shut down in the Labrador Sea (Gelderloos et al., 2011) as interior subsurface water mass properties were warming and becoming more saline matching the lateral input of Irminger Water, while the surface properties were cooling and freshening matching Arctic water input (Straneo, 2006). The baroclinic boundary currents occasionally shed eddies, particularly Irminger Rings, which help restratify the region, supplying upward of 45% of the heat lost during the convective winter (Gelderloos et al., 2011; Saenko et al., 2014). While this is the current understanding of the lateral input during the restratification period, questions remain regarding the relative regional importance of the slow restratification process.

The addition of freshwater into the interior of the Labrador Sea has a strong impact on deep convection. As the stratification determines how much buoyancy must be removed for convection to occur, an input of freshwater which increases stratification can reduce convection and subsequent water mass transformation (Avisc et al., 2006; Fischer et al., 2010). While the boundary currents carry freshwater in the liquid phase, sea ice can play an important role as well. The interior of the Labrador Sea remains relatively ice free, though ice is produced in the northern basin and advected along the Labrador Coast (Close et al., 2018). Sea ice can be advected or blown toward the warmer interior region, supplying freshwater via melting (Close et al., 2018; McGeehan & Maslowski, 2011), influencing the stratification within the convective region. The input of a sufficient amount of freshwater may strengthen the stratification such that the buoyancy loss via atmospheric cooling cannot result in convection (Schmidt & Send, 2007). During the 1960s, a large amount of Arctic water reached the Labrador Sea, an event later called a Great Salinity Anomaly (Belkin et al., 1998; Dickson et al., 1988; Gelderloos et al., 2012). The combination of additional freshwater from the Great Salinity Anomaly and weak atmospheric forcing produced multiple years with a shutdown in deep convection (Gelderloos et al., 2012). While a massive input of freshwater over a short period has been shown to limit Labrador Sea convection, numerical simulations suggest that a gradual increase in the freshwater input to the Labrador Sea alone could shut down convection (Böning et al., 2016) and stop the production of Labrador Sea Water (LSW).

A reduction in LSW formation has implications on the Atlantic Meridional Overturning Circulation (AMOC). While measurements made in the 1990s (Pickart & Spall, 2007) suggest that the northward transport within the AMOC is not strongly affected by deep convection within the Labrador Sea, Böning et al. (2016) investigated how runoff from Greenland affected convection within the Labrador Sea and the strength of the AMOC. Using numerical simulations, they found that, under current Greenland melting rates estimated for the near future, enough freshwater could reach the convection region within the Labrador Sea, build sufficient stratification to prevent deep convection and LSW formation, and significantly reduce the northward AMOC transport. However, the impact of LSW production and the AMOC is still being investigated, as recent research suggests that deep water formation within the eastern North Atlantic plays a much stronger role than that within the Labrador Sea (Chafik & Rossby, 2019; Lozier et al., 2019).

This study seeks to further understand the net freshwater transport between the boundary currents and the interior of the Labrador Sea. We put emphasis on regions around the western portion of the North Atlantic subpolar gyre (Figure 1d) which have cross-shelf freshwater transport, either onshore or offshore, across multiple isobaths ranging in depth from 500 to 2,000 m. Stratification is not only dependent on the surface freshwater, so three water masses are selected for freshwater transport quantification: fresh water from polar origins, salty and warm water of Atlantic origins, and salty and cold LSW. This allows for increased understanding and quantification regarding regions which act to supply or sequester freshwater/saltwater from the interior of the Labrador Sea. The influence of mesoscale features, including eddies, on freshwater transport is also investigated by decomposing the total freshwater transport into the mean and turbulent components.

2. Methods

To examine the amount of fresh and saline water that enters the interior of the Labrador Sea, we perform three simulations using the Nucleus for European Modelling of the Ocean (NEMO), version 3.4 (Madec, 2008), coupled with the Louvain-La-Neuve sea ice model (LIM 2, Fichefet & Maqueda, 1997). We use a regional ORCA configuration (Barnier et al., 2007), called ANHA (Arctic Northern Hemisphere Atlantic; Hu et al., 2018; Grivault et al., 2018; Holdsworth & Myers, 2015; Müller et al., 2017; Courtois et al., 2017) at both 1/4° horizontal resolution (ANHA4; Figure 1a), as well as 1/12° resolution (ANHA12; Figure 1b). A third simulation uses the ANHA4 configuration with a 1/12° nest (Figure 1c) over the North Atlantic subpolar gyre (SPG12; Müller et al., 2017), using the Adaptive Grid Refinement In FORTRAN (AGRIF; Debreu et al., 2008) package. The SPG12 nest uses a 3–1 horizontal ratio between the number of nested grid points and the parent grid points over the same region. Two-way feedback is used to allow communication from the parent domain to the nest along the boundary, as well as from the nest back to the parent for all nested points. All simulations use a geopotential vertical coordinate with 50 levels where nine model levels fit within the top 10 m and our last level is 458 m thick. Even at 1/12° horizontal resolution, regions exist around the Labrador Sea which would not be considered eddy resolving due to a small baroclinic Rossby radius in these waters (see Müller et al., 2019, Figure 2c), so one should consider the 1/12° simulations to be eddy

Table 1
Configuration Settings for Each Given Simulation

	Resolution	Time step	Eddy viscosity	Eddy diffusivity	Computing cost
	(°)	(s)	(m^4/s)	(m^2/s)	(core years)
ANHA4	1/4	1,080	1.5×10^{11}	300	0.75
ANHA12	1/12	180	1.0×10^{10}	50	13
SPG12	1/12	180	1.0×10^{10}	50	2

Note. One core year is the amount of computation that would occupy a single core for 365 days.

permitting, bordering on eddy resolving. All three simulations share identical forcing and parameters, except for the time step, horizontal resolution, and time step-dependent values (Table 1). Horizontal advection was carried out using a total variance dissipation scheme (Zalesak, 1979), while lateral diffusion used a Laplacian operator. A biLaplacian operator was used for lateral momentum mixing. Model mixed layer depths were calculated using a 0.01 kg/m^3 change in potential density from the surface. This method can produce mixed layer depths which are deeper than water properties suggest in this region as Courtois et al. (2017) found. Furthermore, Courtois et al. (2017) identify that their NEMO simulations of varying resolution share some distinct spatial and vertical scales of the mixed layer (their Figure 8). Part of this may be due to biases linked to the freshwater within the boundary currents (Rattan et al., 2010; Tréquier et al., 2005) which then is exported toward the convection region, influencing the mixed layer depth. However, others find that resolving Irminger Rings dramatically improve the representation of convection due to the significant buoyancy provided by these eddies (Gelderloos et al., 2011), though this requires high spatial resolution and coarser resolution simulations may suffer.

Our simulations were forced with the Canadian Meteorological Centre's Global Deterministic Prediction System (Smith et al., 2014), using hourly 2-m temperature, precipitation, downwelling longwave and shortwave radiation, 2-m specific humidity, and 10-m zonal and meridional wind velocity. Interannual monthly runoff was remapped from 1° gridded data (Dai et al., 2009) to the configuration grid. Liquid runoff from Greenland was further improved by remapping the surface mass balance from a regional climate simulation (Bamber et al., 2012) onto the ocean model grid with a volume conservation approach. Without an iceberg module coupled with NEMO at the starting time of our simulations, solid discharge was ignored. Initial conditions of sea surface height, temperature, salinity, and horizontal velocities were obtained from the year 2002 from GLORYS2v3 (Ferry et al., 2010), a global ocean configuration with horizontal resolution of 1/4° and the same horizontal grid (ORCA) as our regional NEMO simulations. Boundary conditions of temperature, salinity, and velocity at Bering Strait and 20°S latitude were also obtained from GLORYS2V3. Bathymetry was interpolated from ETOPO GEBCO (Amante & Eakins, 2009) for the ANHA4 simulation, while ANHA12 used bathymetry from Smith and Sandwell (1997) except over the Arctic Ocean where ETOPO GEBCO was used. Little difference (not shown) was noted between these two bathymetric data sets. All simulations were integrated from 2002 until the end of 2016, and model output was exported as 5-day averages, producing 73 output periods per model year. As 3-D initial velocities were prescribed from GLORYS2v3, each simulation was considered already spun-up. However, we allowed each simulation 4 years of adjustment from the initial conditions; all analysis took place between 2006 and 2016.

To calculate cross-isobath freshwater transport, a reference salinity, *Sref* (equation (1)), of 34.8 was used, consistent with the literature focused on the Labrador Sea (e.g., Aagaard & Carmack, 1989; Cuny et al., 2005; Curry et al., 2014). Multiple regions around the subpolar gyre are constructed (Figure 1d) to determine regional freshwater transport. We decompose the total velocity into mean and turbulent components (equations (2) and (3)) to quantify how the turbulent freshwater transport differs from the mean freshwater transport. To determine the average velocity (u_{ave}, v_{ave}), a 25-day moving average was performed on both the meridional (v) and zonal (u) velocities. To determine the turbulent velocity, the meridional and zonal velocities were subtracted from the 25-day moving average. Other moving average windows were examined (not shown), though the 25-day moving average gave the highest turbulent transport values indicating that the mean velocity is changing significantly at time scales of nearly 1 month. While calculation of freshwater via individual eddies could be carried out, we chose to calculate the flow which deviated from the 25-day moving average as this would contain any contribution from short time scale features: We call this the turbulent transport. As the simulations are not fully eddy resolving, the subgrid scale physics should produce the effect of eddies and turbulence to some degree while not explicitly resolving these eddies and their associated transport.

We calculate the freshwater flux by integrating horizontally and vertically along each region's isobath using the grid cell's salinity and velocity normal to the horizontal path of integration (equation (4)). Five isobaths were used: 500, 750, 1,000, 1,500, and 2,000 m (see Figure 1d). Freshwater calculations include both water

fresher than the reference salinity and water which was saltier. The direction of freshwater transport is defined to be positive if there was fresher water transported into the interior of the subpolar gyre, or if saltier water was transported toward the shore. The direction of freshwater transport will henceforth be called an *import* if there was freshwater (saline water) transported onshore (offshore), and an *export* for freshwater (saline water) transported offshore (onshore).

$$\mathrm{FW} = (\mathrm{Sref} - \mathrm{Salinity})/\mathrm{Sref} \tag{1}$$

$$\text{Mean velocity} = \sqrt{(u_{\mathrm{ave}}{}^2 + v_{\mathrm{ave}}{}^2)} \tag{2}$$

$$\text{Turbulent velocity} = \sqrt{\left[(u_{\mathrm{ave}} - u)^2 + (v_{\mathrm{ave}} - v)^2\right]} \tag{3}$$

$$\text{Cross isobath freshwater flux} = \int_0^L \int_0^z \mathrm{FW}^* \text{velocity}\, dz\, dl \tag{4}$$

To determine if the freshwater transport is due to the flow of water which is fresher or more saline than our reference salinity, we partition the transport into three water masses: cold and fresh Polar Water, warm and salty Irminger Water, and cold and salty LSW. By selecting multiple water masses we can better understand where freshwater exchanges between the shelf and the interior, further addressing open questions regarding lateral exchange and restratification in the Labrador Sea. We separate LSW by potential density, from 27.68 to 27.80 kg/m^3 as used by Kieke et al. (2006), with no additional temperature or salinity criteria. The Irminger Water mass was chosen to be warm (>3.5 °C) and salty (>34.8), but with density less than LSW. We selected a lower salinity criteria for Irminger Water than traditionally used (see Myers et al., 2007) so there would be no gap in freshwater transport between Polar Water and Irminger Water. While we could have called this water mass Atlantic Water or some variant of, we felt it was important to keep the name closely attached to the water within the boundary current which has a strong impact on restratification. Polar Water was selected to be less dense than 27.68 kg/m^3, with salinity below 34.8, consistent with previous studies (de Steur et al., 2017; Sutherland & Pickart, 2008), and for any temperature range. These three water masses do not encompass all water within the Labrador Sea, such as the overflow waters of Iceland-Scotland (Swift, 1984) and Denmark Strait (Jonsson & Valdimarsson, 2004), though they encompass the water masses which influence the stratification that must be eroded before deep convection begins. Figure 2 illustrates the various water masses within Atlantic Repeat Hydrography Line 7 West (AR7W) at a snapshot during the simulation. Due to the vertical grid and the AR7W section which is not orthogonal to the model grid, a stair step pattern emerges in the horizontal and vertical dimensions. The large vertical changes between the boundary of LSW and that which is underneath is simply a consequence of our selection criteria and how they deviate over one model grid, which is around 250 m thick at 1,500 m of depth.

One caveat of the above water mass selection criteria is that we are unable to state the specific origin of each water parcel as it crosses the shelf break. For example, transport along the western slope of Greenland may include fresh glacial melt, East and West Greenland Current water, Irminger Water, East Greenland Coastal Current water, and more. While interesting, it is beyond the scope of this manuscript which seeks to quantify the regional fresh and salt water transport between the shelf and interior basin that impacts the stratification within the Labrador Sea.

To determine regional differences in the freshwater transport to the interior of the Labrador Sea, six different geographic regions were selected: the east coast of Greenland, the west coast of Greenland, the Davis Strait region, the Hudson Strait region, the northern coast of Labrador, and the southern coast of Labrador (Figure 1d). As ANHA4 and ANHA12 used slightly different bathymetry data, and are different in horizontal grid resolution, the isobaths depicted in Figure 1d would appear slightly different for the ANHA4 simulation. The bathymetry for ANHA12 and SPG12 are identical other than within the sponge layer of SPG12 as that is a combination of the ANHA12 bathymetry and the corresponding parent (ANHA4) grid cell's bathymetry.

3. Model Evaluation

The ANHA12 simulation has been used in several previous studies, including examining sea ice thickness in the Canadian Arctic Archipelago (Hu et al., 2018) and the importance of surface stresses due to ice motion in the Canadian Arctic Archipelago (Grivault et al., 2018). A previous ANHA12 simulation with slightly

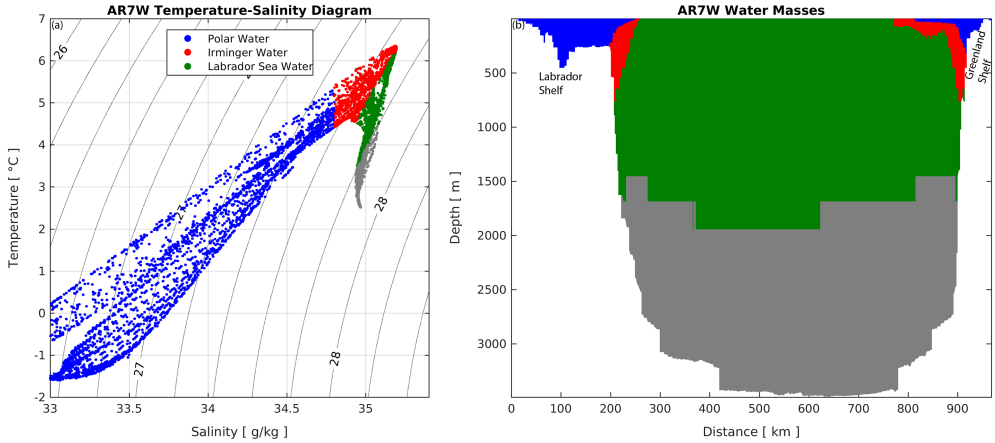

Figure 2. Model snapshot for 5 May 2009, across AR7W depicting the temperature-salinity graph (a) and cross-section profile (b). Three water masses are shown: Polar Water (blue) with any value for potential temperature, salinity less than 34.8, and potential density less than 27.68 kg/m^3; Irminger Water (red) with potential temperature above 3.5 °C, salinity above 34.8, and potential density less than 27.68 kg/m^3; Labrador Sea Water (green) with any value for potential temperature or salinity, but with potential density between 27.68 and 27.8 kg/m^3.

different settings was used to examine the mixed layer depth within the Labrador Sea (Courtois et al., 2017), mixing in the Canadian Arctic Archipelago (Hughes et al., 2017), and meltwater pathways from Greenland's glaciers (Gillard et al., 2016). However, further comparison against observations is necessary to quantify the model's fidelity within the Labrador Sea.

To evaluate our simulation, we first compare some model processes against observations within the Labrador Sea. To determine if the temperature and salinity field is comparable to observations, bottle data from four different AR7W (see Figure 1d) occupations (CCGS *Hudson*: 2002, 2006, 2010, and 2013) are plotted against model data (Figure 3a). At first glance, the model appears in close alignment with observations, though some model drift appears present. Model drift of the salinity field is a known issue in regards to numerical simulations within the North Atlantic subpolar gyre (e.g., Rattan et al., 2010; Tréquier et al., 2005). This long-term issue is still present, as Marzocchi et al. (2015) recently discussed salinity drift within the Labrador Sea with a high resolution 1/12° NEMO simulation. While our three model simulations exhibit drift (not shown but discussed below), the comparison against observations is reasonable, and the temperature, salinity, and thus density field of the Labrador Sea is reliable.

Geostrophic current speed derived from Archiving, Validation and Interpretation of Satellite Oceanographic data (AVISO, http://www.aviso.altimetry.fr/duacs/) are subtracted from ANHA12 (Figure 3b) for the period from 2006 to 2015. Due to different resolution and grid spacing, and interpolating the ANHA12 data onto the same grid as AVISO, some spatial differences are anticipated. Swift boundary currents around the Labrador Sea contain much higher discrepancies than that of the quiescent interior. A likely culprit arises from issues with altimetry products close to the coast or near ice, impacting the AVISO derived speed. However, some spatial discrepancies occur along the shelf-break, perhaps due to differences in the spatial placement of the boundary current between the observation product and the ANHA12 simulation. Regardless of the cause, the ANHA12 simulation produces slightly faster boundary currents than observations derived via satellite, though the satellite product has higher variability in these regions, as we show below.

Eddy kinetic energy (EKE: $0.5\left(\overline{U_g'^2}+\overline{V_g'^2}\right)$), where U_g' and V_g' are the geostrophic velocities computed from the sea surface height anomaly (see Jia et al., 2011), is calculated from the AVISO data set (Figure 3c) and ANHA12 simulation (Figure 3d). As shown in this image, the Northwest Corner has the highest EKE, upward of 1,000 cm^2/s^2. Other noticeable regions with strong EKE are along the western side of Greenland, a location where Irminger Rings are shed, and along the Labrador Shelf. Similarities emerge between the ANHA12 simulation and AVISO. First, the Northwest Corner has a similar spatial extent where the maximum in observed EKE exists, though the ANHA12 simulation has an extension of high EKE to the northwest. The high observed EKE values off the west coast of Greenland are shifted northward in ANHA12

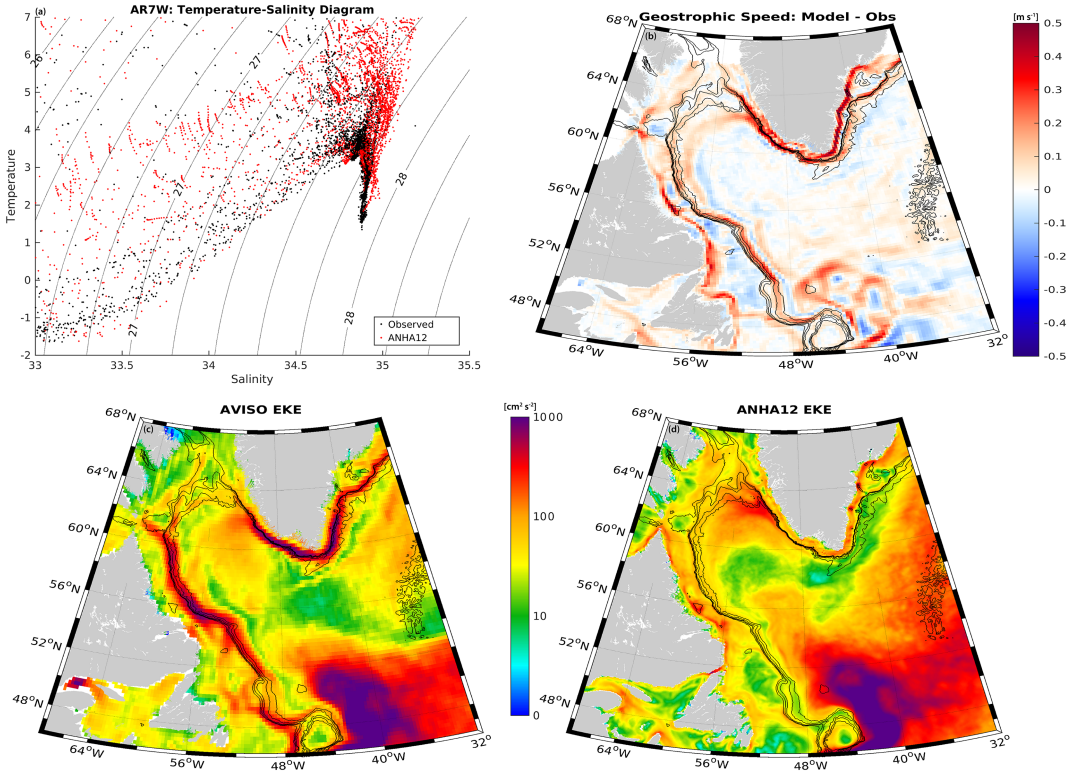

Figure 3. (a) Temperature-salinity graph across AR7W (dotted line in Fig 1.d) comparing bottle data from four CCGS *Hudson* cruises (2002, 2006, 2010, and 2013: black) against ANHA12 (red). Mean geostrophic velocities difference between ANHA12 and AVISO from 2006–2015 are shown in (b). AVISO-derived eddy kinetic energy (cm^2/s^2) from 2006–2015 is shown in (c) and the same for ANHA12 (d). ANHA = Arctic Northern Hemisphere Atlantic.

and do not penetrate south into the interior of the Labrador Sea but instead follow the isobaths around the Labrador Sea. While the EKE signatures off this coast are comparably different than observations, the modelled EKE values suggest high levels of eddy activity which are observed nearby. The strong boundary currents along Greenland and the Labrador coast show high levels of observed EKE, while the model does not quite capture it, often having higher EKE closer to shore. This is likely a result from multiple features. First, altimetry products tend to have inaccuracies at coastal regions and near sea ice (see Volkov et al., 2007), leading to inaccuracies in EKE along the coast and in regions where sea ice is present, including the Labrador Shelf. Second, while coarser in spatial resolution, the observation product includes higher variability of the geostrophic flow and produces higher EKE where the simulation does not. This is not surprising as many numerical simulations have lower EKE than observations (e.g., Luo et al., 2011). However, we note that regions which experience high EKE are also simulated with elevated levels of EKE. Third, numerical simulations within the Labrador Sea may produce the western boundary current to be too barotropic (Handmann et al., 2018) and likely reduces the baroclinic instability that influences the eddy field in this region (Rieck et al., 2019). Our 1/12° simulations are not fully eddy resolving, and some small-scale features will instead be resolved as part of the mean flow, reducing the EKE in some regions. Fortunately, our 1/12° simulations are able to resolve Irminger Rings (not shown), eddies which divert substantial heat flux to the interior of the Labrador Sea (Gelderloos et al., 2011), a critical component of the restratification season. As the EKE mismatch between observations and model is elevated along the shelf-break, we anticipate some reduction in the eddy fluxes across these regions. However, this reduction should increase the mean freshwater transport while the net freshwater transport, the primary objective of this study, should remain unchanged. Thus, we have some degree of confidence in the ability for the ANHA12 simulation to represent eddy fluxes within the Labrador Sea, though we anticipate the observed eddy fluxes would be stronger than our simulations suggest.

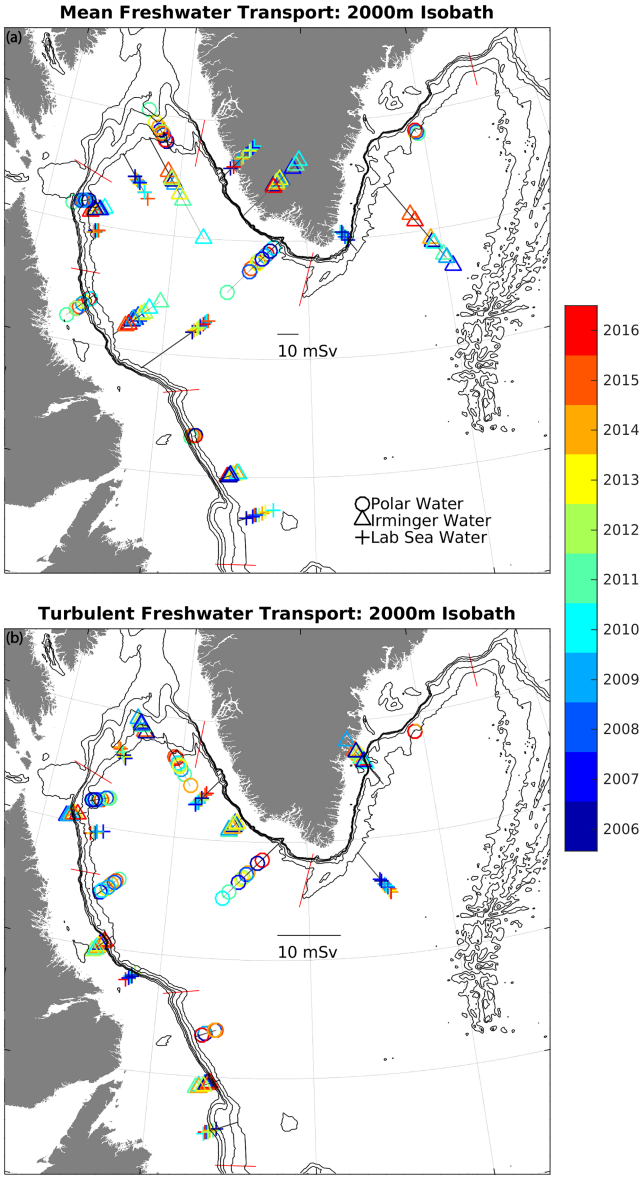

Figure 4. Yearly mean (a) and turbulent (b) freshwater transport crossing the 2,000-m isobath of the North Atlantic subpolar gyre. Three water masses are used: Polar Water (O), Irminger Water (△), and Labrador Sea Water (+). The distance from the isobath determines freshwater strength, with a 10-mSv sample line illustrated. Values that are directed off-shore indicate a freshening of the Labrador Sea via the given water mass.

Some limitations based on the evaluation above should be expressed. First, our 1/12° simulations are not fully eddy resolving and may have different freshwater transport via eddy processes than observations may suggest, based on EKE differences. The differences between modelled and observed EKE may be due to our choice of lateral boundary conditions, set as free-slip, as simulations which feature partial-slip or no-slip are more likely to produce eddies and propagate offshore (Quartly et al., 2013). However, part of this manuscript identifies the differences between our high resolution simulations and low-resolution simulation, quantifying each, and understanding if horizontal resolution matters when it comes to cross-shelf freshwater transport in the Labrador Sea. And second, model drift can play an important role when differentiating between water masses, since salinity and temperature drift will also impact the density. A slight change in either the salinity or density via our classifications can push water into a different classification. We investigated salinity drift within our ANHA4 simulation by quantifying the salt content within a section from Cape Farwell extending south to the 2,500-m isobath. Salt content of our three water masses identify (not shown) that while the entire section gradually gains in salt, the interannual variability (20–50%) greatly exceeds that of the slow increase in total salt (<0.5%) during the 2006–2015 analysis period. Furthermore, even with some model drift present, the ANHA12 simulation generally produces LSW within the observed density range (see Figure 5 by Feucher et al., 2019) indicating the drift over our simulation length still results in accurate LSW properties. Under such circumstances, we decided to keep our water mass classifications constant in time rather than allow for water mass evolution taking model drift into account.

4. Results

4.1. Regional Freshwater Transport

The net mean and turbulent freshwater transport from the ANHA12 simulation is shown in a spatial-temporal manner (Figure 4), characterizing the annual freshwater transport across the 2,000-m isobath within each region. The deepest isobath was selected as some of the freshwater crossing this isobath may penetrate further into the interior of the Labrador Sea, impacting deep convection. The west coast of Greenland and the Davis Strait region are particularly active in terms of freshwater transport for all three water masses, while the southern coast of Labrador and Hudson Strait are fairly quiescent. While the direction of mean freshwater transport varies across the regions, turbulent freshwater transport is generally offshore (Figure 4b). Other than a few regions where transport is very low, neither the transport associated with the mean velocity nor the turbulent velocity shifts direction during the course of the simulation. Furthermore, we can identify regions which have little or no transport by select water masses. For example, the east coast of Greenland has essentially no Polar Water exchange across the 2,000-m isobath. The turbulent freshwater transport is relatively low across most of the regions and isobaths around the subpolar gyre. As such, most of the remaining figures will illustrate the total freshwater transport, while the mean and turbulent freshwater transport, as well as their standard deviations, are shown in Table 2. Almost all regions experienced fresh/saltwater transport which was significantly different from 0, as determined by a Student's *t* test at the 0.05 alpha level (bold values in Table 2). Henceforth, discussion of results will be carried out for regions where the freshwater transport, via either mean or turbulent transport, is strong or seasonally variable. While Figure 4 identifies spatial regions with varying freshwater transport across a single isobath, no seasonal variation is shown. A description of the ANHA12 simulation's cross-isobath freshwater transport for multiple regions of the North Atlantic subpolar gyre follows below.

4.2. Polar Water Mass

The net liquid freshwater transport associated with Polar Water crossing various isobaths along the east coast of Greenland is shown in Figure 5 (black bars). Little freshwater exchanges along this coast regardless of the isobath examined, with a maximum around 5 mSv. This appears a result of the mean and turbulent flow (Table 2) acting in opposite directions with a similar magnitude of freshwater transport. The total freshwater transport by liquid and sea ice is indicated by the black dots in Figure 5. Sea ice almost always supplies freshwater toward the interior basin. While only a few regions experience freshwater transport via sea ice across the 2,000-m isobath (Figure 5e), it is possible that sea ice melt makes its way into the deeper basin as Close et al. (2018) suggest.

While little freshwater was exchanged along the eastern coast of Greenland via both liquid and solid transport, the western coast of Greenland (Figure 5; red bars) has significant offshore liquid freshwater transport (5–70 mSv), though only a small amount of freshwater is exchanged via sea ice (<5 mSv). The freshwater transport changes significantly month to month, with a minimum in freshwater export during the summer and a maximum during the winter. Similar to the east coast of Greenland, the magnitude of freshwater transport generally decreases across deeper isobaths. Seasonality is strong here such that winter months have upward of 3 times as much freshwater export as summer months. From observations, Schmidt and Send (2007) estimated freshwater transport between the West Greenland Current and the interior of the Labrador Sea to be around 24 mSv which coincided with a pulse of freshwater within the West Greenland Current between April and September. Rykova et al. (2015) used observations to state that the April–September period held a thicker and fresher amount of Polar Water within the West Greenland Current, which thinned during the typically unobserved winter period. Our results suggest that the total freshwater transported across the 2,000-m isobath during April was about 30 mSv, while September was about 10 mSv. Observations suggest this 6-month offshore transport can vary between 11 (Khatiwala et al., 2002) and 30 mSv (Lazier, 1980) making our ANHA12 simulation appearing in good agreement. Schulze and Frajka-Williams (2018) used Lagrangian particle tracking software and found that while March had the highest number of particles crossing from the western coast of Greenland into the interior of the Labrador Sea, the winter months also had high transport, further agreeing with our findings. This region also experiences significant freshwater transport due to turbulent features (Figure 6a), as most isobaths export freshwater toward the interior basin (Luo et al., 2016; Schulze & Frajka-Williams, 2018). Turbulent freshwater export appears heightened during the winter period, from December to April, likely Ekman driven from enhanced wind stress (Schulze & Frajka-Williams, 2018). A significant amount of the freshwater transport within this water mass as it flows past Cape Desolation is exported from the western coast of Greenland into the deep basin (Figure 7). The alongshore freshwater transport corresponds rather well against the offshore freshwater transport across the 500- ($r^2 = 0.71$) and 2,000-m ($r^2 = 0.49$) isobaths of the western coast of Greenland, suggesting that an increase in alongshore transport will result in an increase in offshore transport within this region.

The Davis Strait region (Figure 5; magenta bars) exports freshwater across the shallow 500- and 750-m isobaths, while importing freshwater from across the remaining isobaths. The largest import of freshwater (5 to 30 mSv) occurs across the 1,000-m isobath. The nearby 750-m isobath has considerably different freshwater transport, exporting between −2 and 10 mSv. The deeper isobaths have higher seasonality than the shallow isobaths, with a minimum in freshwater import during the summer season and a maximum during winter. Considering how the shallow isobaths show a similar pattern associated with the export of freshwater, we suspect this is due to additional offshore transport across all isobaths, though not nearly enough to counter the import occurring between 1,000 and 2,000 m. While the liquid component shows a split of import and export across the five isobaths, sea ice only exports freshwater consistent with the above regions as well as those to be later described. Sea ice carries up to 10 mSv of freshwater transport, far more than upstream Greenland coast regions. While Davis Strait has a history of observations (Cuny et al., 2005; Curry et al., 2011), the isobaths selected here exist too far south of the mooring array to be comparable.

The Hudson Strait region is characterized by freshwater import (Figure 5; yellow bars) across all but the 1,500-m isobath, with monthly import rates between 30 and −10 mSv. The strongest import occurs at the shallowest isobath, while the deep isobaths have weak transport. Hudson Strait experiences monthly variability with a minimum import rate during the late spring and early summer, though a maximum is reached at different times depending on the isobath. Relatively few similarities emerge between the Davis Strait and

Journal of Geophysical Research: Oceans

10.1029/2019JC015144

Table 2
Freshwater Transport (mSv) for Each of the Three Water Masses, for All Six Regions, Across All Five Isobaths

Section	Water mass	FW component	500 m		750 m		1,000 m		1,500 m		2,000 m	
			Export	Import	Export	Import	Export	Import	Export	Import	Export	Import
East Greenland Coast	Polar	Mean [sd]		**7.8 [4.1]**		**3.6 [2.4]**		**1.1 [1.7]**	**0.6 [0.8]**		**0.6 [0.6]**	
		Turbulent [sd]	**6.0 [2.2]**		**3.4 [1.3]**		**2.5 [0.9]**		**1.3 [0.6]**		**0.0 [0.1]**	
	Irminger	Mean [sd]	1.7 [3.5]		**16.8 [2.6]**		0.3 [2.0]			1.2 [2.8]	**37.4 [9.4]**	
		Turbulent [sd]		**1.3 [1.2]**		**5.3 [0.7]**		**2.3 [0.5]**	**1.8 [1.2]**			**6.1 [1.3]**
	LSW	Mean [sd]	**9.5 [12.0]**		**2.7 [3.9]**			**32.4 [10.7]**		**34.9 [3.9]**		**9.1 [1.9]**
		Turbulent [sd]		**1.6 [0.8]**		0.3 [0.8]	**4.7 [1.7]**		**8.9 [0.9]**		**7.2 [0.9]**	
West Greenland Coast	Polar	Mean [sd]	**44.0 [12.0]**		**27.2 [11.5]**		**32.1 [10.7]**		**30.1 [12.8]**		**13.3 [8.4]**	
		Turbulent [sd]	**1.7 [0.5]**		**10.3 [2.7]**		**7.7 [2.2]**		**6.7 [2.3]**		**7.6 [2.5]**	
	Irminger	Mean [sd]		**6.7 [0.9]**		**28.1 [2.4]**		**39.9 [3.7]**		**51.9 [7.8]**		**26.6 [6.0]**
		Turbulent [sd]	**3.4 [0.5]**		**11.4 [1.2]**		**12.8 [1.6]**		**11.1 [1.9]**		**1.7 [0.6]**	
	LSW	Mean [sd]	0.0 [0.0]		0.0 [0.4]			**8.8 [9.1]**		**19.3 [5.1]**		**17.1 [5.1]**
		Turbulent [sd]	0.0 [0.0]		0.0 [0.1]		**19.3 [7.0]**		**6.4 [1.2]**		**4.2 [0.8]**	
Davis Strait	Polar	Mean [sd]	**13.0 [3.9]**		**9.4 [3.3]**			**18.8 [5.0]**		**10.6 [4.8]**		**11.0 [4.8]**
		Turbulent [sd]		**2.8 [1.6]**		**3.1 [1.2]**	0.6 [1.1]		**1.3 [1.3]**		**2.6 [1.5]**	
	Irminger	Mean [sd]		**0.3 [0.2]**		**2.4 [0.6]**	**17.6 [6.1]**		**21.5 [6.5]**		**27.7 [10.0]**	
		Turbulent [sd]	**0.5 [1.2]**		**1.6 [0.3]**			**0.9 [0.3]**		**2.8 [0.9]**		**2.5 [0.8]**
	LSW	Mean [sd]	0.0 [0.0]			0.1 [0.1]		**4.6 [6.1]**	**12.2 [2.4]**		**16.8 [3.7]**	
		Turbulent [sd]	0.0 [0.0]		**0.0 [0.0]**		**3.5 [4.1]**			**3.9 [1.2]**		0.2 [0.7]
Hudson Strait	Polar	Mean [sd]		**30.9 [7.2]**		**17.5 [6.0]**		**9.4 [4.3]**		**1.5 [1.8]**		**3.0 [2.1]**
		Turbulent [sd]	**8.1 [1.3]**		**6.7 [1.4]**		**5.5 [1.3]**		**2.4 [0.9]**		**1.7 [1.0]**	
	Irminger	Mean [sd]	**1.6 [0.5]**		**2.2 [0.6]**		**1.1 [0.8]**			**5.6 [1.9]**	**5.3 [2.0]**	
		Turbulent [sd]		**0.2 [0.1]**		**0.6 [0.2]**		**0.4 [0.1]**	**1.2 [0.5]**			**2.4 [0.5]**
	LSW	Mean [sd]	0.0 [0.0]			**0.2 [0.2]**		**7.6 [3.0]**		**9.0 [1.3]**	**2.2 [0.7]**	
		Turbulent [sd]	0.0 [0.0]		**0.0 [0.0]**		**3.2 [1.5]**		**3.8 [0.4]**		**0.6 [0.5]**	
North Labrador Coast	Polar	Mean [sd]		**25.4 [6.5]**		**27.0 [7.8]**		**21.1 [7.2]**		**13.0 [5.9]**		**7.0 [4.5]**
		Turbulent [sd]	**15.0 [2.6]**		**13.2 [2.7]**		**10.7 [2.5]**		**5.0 [1.5]**		**2.8 [1.3]**	
	Irminger	Mean [sd]		**0.8 [0.2]**	**4.8 [2.1]**		**6.2 [2.6]**		**15.8 [5.2]**		**15.3 [5.7]**	
		Turbulent [sd]	**0.6 [0.1]**		0.1 [0.2]			**0.2 [0.3]**		**1.9 [0.4]**		**2.8 [0.8]**
	LSW	Mean [sd]	0.0 [0.0]		**0.9 [0.7]**			0.5 [7.9]	**20.0 [3.1]**		**34.3 [2.9]**	
		Turbulent [sd]	0.0 [0.0]		**0.0 [0.0]**			0.9 [7.1]		**0.7 [0.3]**		**1.9 [0.5]**
South Labrador Coast	Polar	Mean [sd]		**5.5 [2.8]**		**1.1 [1.4]**	**0.9 [1.1]**		**1.8 [1.1]**			**0.7 [0.6]**
		Turbulent [sd]	**6.8 [1.7]**		**5.0 [1.5]**		**4.1 [1.4]**		**3.0 [1.2]**		**2.2 [1.1]**	
	Irminger	Mean [sd]	0.2 [0.7]		0.1 [2.7]		1.6 [3.1]		**2.8 [2.0]**		**6.5 [1.9]**	
		Turbulent [sd]	**0.3 [0.2]**			0.2 [0.4]		**1.2 [0.4]**		**2.5 [0.6]**		**2.5 [0.8]**
	LSW	Mean [sd]	0.1 [0.1]		**0.7 [0.4]**			**5.7 [4.2]**		**7.3 [1.9]**	**10.1 [3.5]**	
		Turbulent [sd]	0.0 [0.0]			0.1 [0.1]		1.7 [4.4]		**1.1 [0.6]**		**4.8 [0.6]**

Note. Both the net mean and net turbulent freshwater transport are identified, and the standard deviation (sd) is shown in brackets. Bold values indicate a transport which is statistically significant from 0 at the 0.05 alpha level. An import refers to net freshwater transport onshore, while an export is offshore. Values are from the ANHA12 simulation averaged from 2006 to 2016. ANHA = Arctic Northern Hemisphere Atlantic; LSW = Labrador Sea Water.

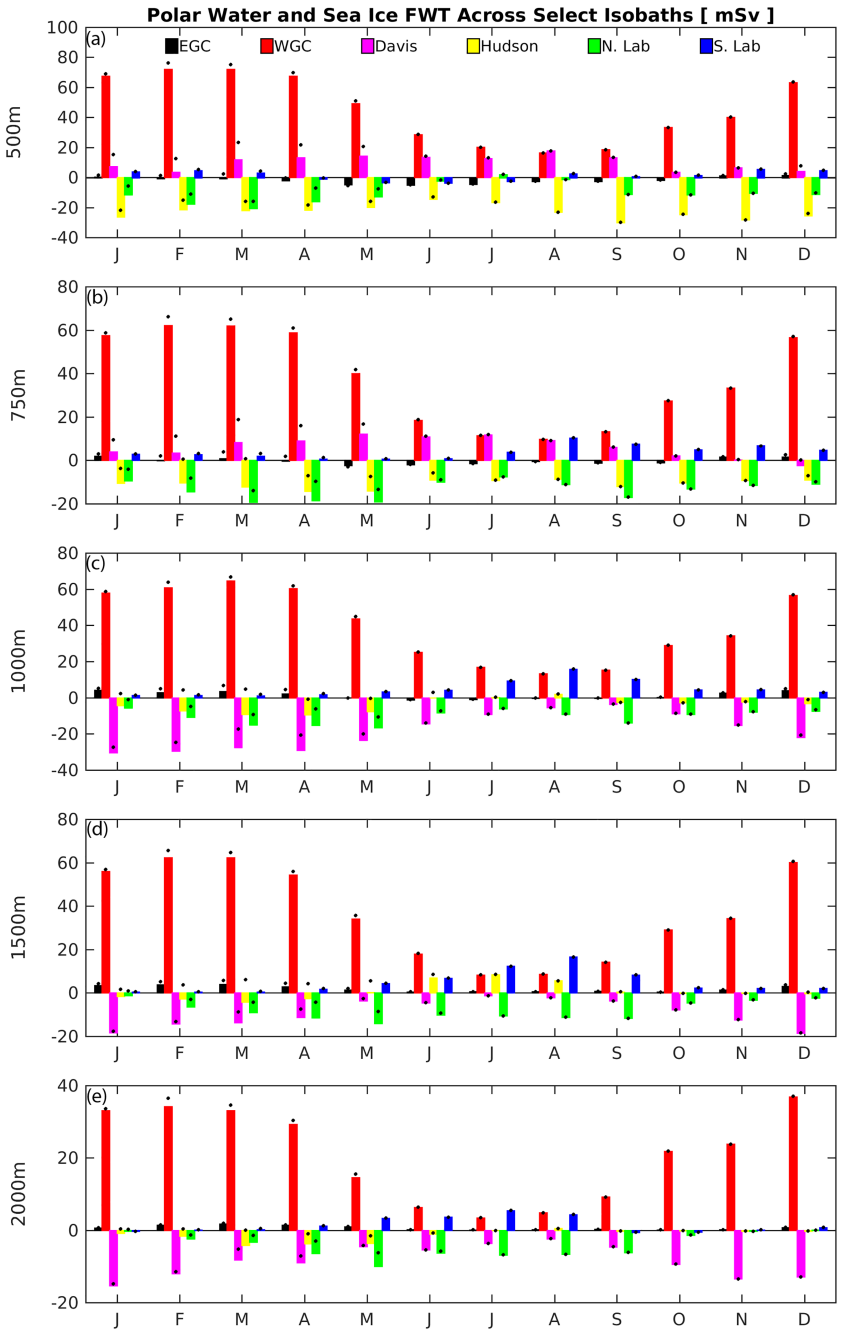

Figure 5. Monthly liquid (bars) freshwater transport (FWT, in millisverdrup) across five isobaths around the North Atlantic subpolar gyre, as simulated by ANHA12 from 2006 to 2016: (a) 500 m; (b) 750 m; (c) 1,000 m; (d) 1,500 m; (e) 2,000 m. Bar colors correspond to the region of interest: black for the eastern coast of Greenland, red for the western coast of Greenland, magenta for Davis Strait, yellow for Hudson Strait, green for the northern coast of Labrador, and blue for the southern coast of Labrador. The total freshwater (liquid and solid) transport at each region is indicated by the black points. Positive values indicate offshore export of freshwater. ANHA = Arctic Northern Hemisphere Atlantic; EGC = East Greenland Coast; WGC = West Greenland Coast.

Hudson Strait regions, suggesting the seasonal variability is likely caused from within Hudson Bay and not upstream. Sea ice export is stronger here than any other region, with up to 15 mSv of freshwater transport. Sea ice freshwater transport is always positive, while the liquid component is generally negative; suggesting that while this region has a general onshore transport of liquid freshwater, the offshore motion of sea ice acts to reduce the net freshwater import. Our Hudson Strait Region exists where observations

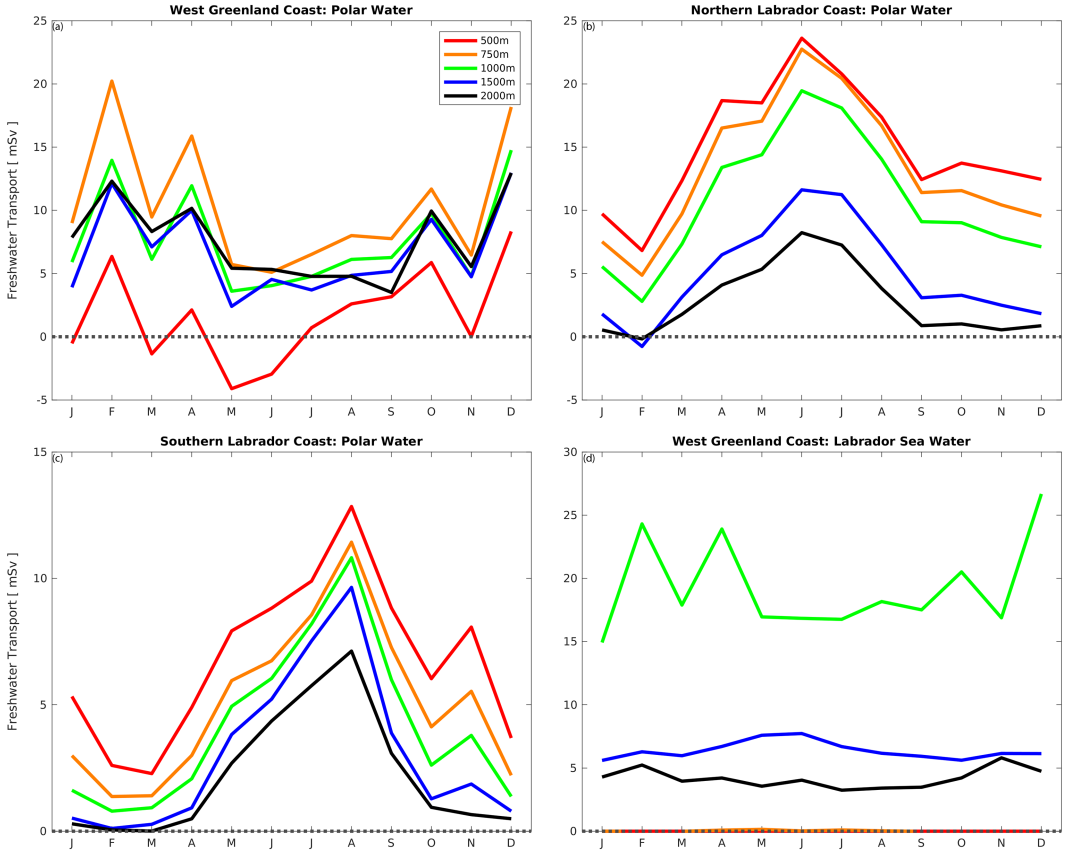

Figure 6. Turbulent freshwater transport for each month as simulated by ANHA12 from 2006 to 2016. Color indicates the isobath in question: red for the 500-m isobath, yellow for 750 m, green for 1,000 m, blue for 1,500 m, and black for 2,000 m. Two water masses are selected: Polar Water at the western coast of Greenland (a), the northern (b) and southern (c) coast of Labrador, and Labrador Sea Water at the west coast of Greenland (d). Positive values indicate an offshore export of freshwater or onshore import of salty water. ANHA = Arctic Northern Hemisphere Atlantic.

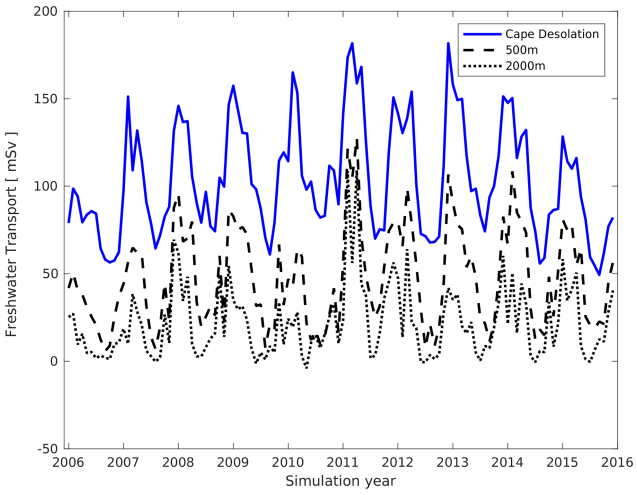

Figure 7. Monthly values for alongshore freshwater transport across Cape Desolation with Polar Water classification (blue), as well as offshore freshwater transport across the 500-m isobath of western Greenland (dash) and the 2,000-m isobath (dotted).

are rather sparse, and, similar to the Davis Strait region above, there exists little comparison between our results and other studies.

The Polar Water mass is characterized by a net import of freshwater (−20 to 2 mSv) across all isobaths of the northern portion of the Labrador coast (Figure 5; green bars). Import rates were higher across the 750-m isobath than 500 m, while deeper isobaths experience decreased import. This region experiences two periods of import maximum and minimum across most isobaths; an import maximum occurs in May and September across the 750-, 1,000-, and 1,500-m isobaths, while a minimum occurs during the late fall and again in the summer. While the 500- and 2,000-m isobaths do not experience two minima and maxima, the monthly variability across the 500-m isobath is similar to the other isobaths while the 2,000-m isobath does not encounter any freshwater change during the springtime. Schmidt and Send (2007) identified two freshwater pulses within the Labrador Current, one from April to May and the other July to August. Our results identify two distinct changes in the freshwater transport that are lagged 1–2 months compared to Schmidt and Send (2007), but both of these pulses still result in a net onshore transport of freshwater. The northern Labrador Coast experiences significant turbulent transport of freshwater (Figure 6b). As the restratification period begins, the density

gradient between the boundary current and the interior of the Labrador Sea peaks, likely promoting exchange with the interior (Straneo, 2006), increasing the offshore turbulent freshwater transport. A clear seasonal cycle is present across all isobaths, with a maximum up to 24 mSv. This matches with McGeehan and Maslowski (2011) who modeled and observed offshore freshwater transport due to eddies in this region. However, with a net freshwater import across the 2,000-m isobath in this region, our simulations match numerical studies including Myers (2005) and McGeehan and Maslowski (2011) in finding that this region supports a net onshore transport of freshwater.

Compared to the northern coast of Labrador, while lower in magnitude, the southern coast (Figure 5; blue bars) is generally characterized by an export of freshwater, also found by both Myers (2005) and McGeehan and Maslowski (2011). The 1,000- and 1,500-m isobaths share similar monthly variability, with freshwater export rates at a minimum during the winter and a maximum during the summer. Freshwater transport generally increases with deeper isobaths, though the 2,000-m isobath has much lower transport compared to 1,500 m. This region of the Labrador Coast shows evidence of a single freshwater pulse identified by Schmidt and Send (2007), taking place between July and August, and unlike the northern coast, this pulse results with a net offshore transport of freshwater, crossing the 2,000-m isobath, resulting in some freshening of the interior of the Labrador Sea. Similar to the northern coast, the southern coast also experiences significant offshore transport of freshwater via turbulent flow (Figure 6c), upward of 12 mSv. The seasonal cycle of turbulent freshwater transport is similar to the northern region, with low export during the fall and winter, though the summer maximum is lagged by 2 months. Turbulent transport of freshwater across the southern coast's 1,000-m isobath (4.1 mSv) is very close in magnitude as well as seasonality when compared to glider observations by Howatt et al. (2018), further strengthening the ability of our simulation to represent reality. While the net offshore freshwater transport that occurs along this coast acts to freshen the Labrador Sea, it does not outweigh the import that occurs along the northern region, implying that the whole Labrador Coast does not provide a net transport of freshwater toward the interior of the Labrador Sea.

4.3. Irminger Water

Heat supplied by Irminger Water acts to restratify the Labrador Sea after the convection period has ceased (Cuny et al., 2002; Lazier et al., 2002; Straneo, 2006), though the salt input helps keep the Labrador Sea weakly stratified and preconditioned for another year of convection. Irminger Water, as defined earlier, is always saltier than our reference salinity and is not a real freshwater source. However, onshore transport of Irminger Water results in an offshore freshwater transport. In this way, Irminger Water can act as a freshwater source, as is the case along the east coast of Greenland (Table 2). However, the east coast of Greenland, along with Hudson Strait and the southern coast of Labrador have, in general, low amounts of freshwater transport and are not illustrated in figures but are presented in Table 2. Furthermore, little seasonal variability exists for this water mass, noted by the low standard deviations within Table 2.

Along the west coast of Greenland (Figure 8; opaque red bars), freshwater is imported along all isobaths via offshore saltwater transport, consistent with an observational study by Myers et al. (2007). The largest amount of Irminger Water is transported across the 1,500-m isobath (34–50 mSv), while similar amounts traverse both the 2,000- and 1,000-m isobaths. Freshwater import tends to increase as the isobath depth increases from 500 to 1,500 m (Table 2). The shallow isobaths between 500 and 1,000 m show limited seasonal variability, though the deeper isobaths experience a maximum during the fall and a minimum during the late winter and spring. This matches well with observations, as Rykova et al. (2015) identified that the Irminger Water thickens and becomes saltier between October and February. Significant amounts of freshwater are exported via turbulent processes in this region between the 750- and 1,500-m isobaths (Table 2), though with limited seasonality as indicated by low standard deviations.

A significant amount of freshwater export occurs along the Davis Strait region via onshore transport of this saline water mass (Figure 8; opaque magenta bars). Upward of 40 mSv crosses the 2,000-m isobath during the fall, while a minimum occurs during spring. The 1,000- and 1,500-m isobaths show similar magnitude of transport as well as seasonality. Unlike the western coast of Greenland, there is essentially no net freshwater transport across the 500- and 750-m isobaths (Table 2).

Similar to the Davis Strait region, Irminger water provides an export of freshwater via onshore transport along the northern coast of Labrador (Figure 8; opaque green bars). While the 1,000-m isobath has low

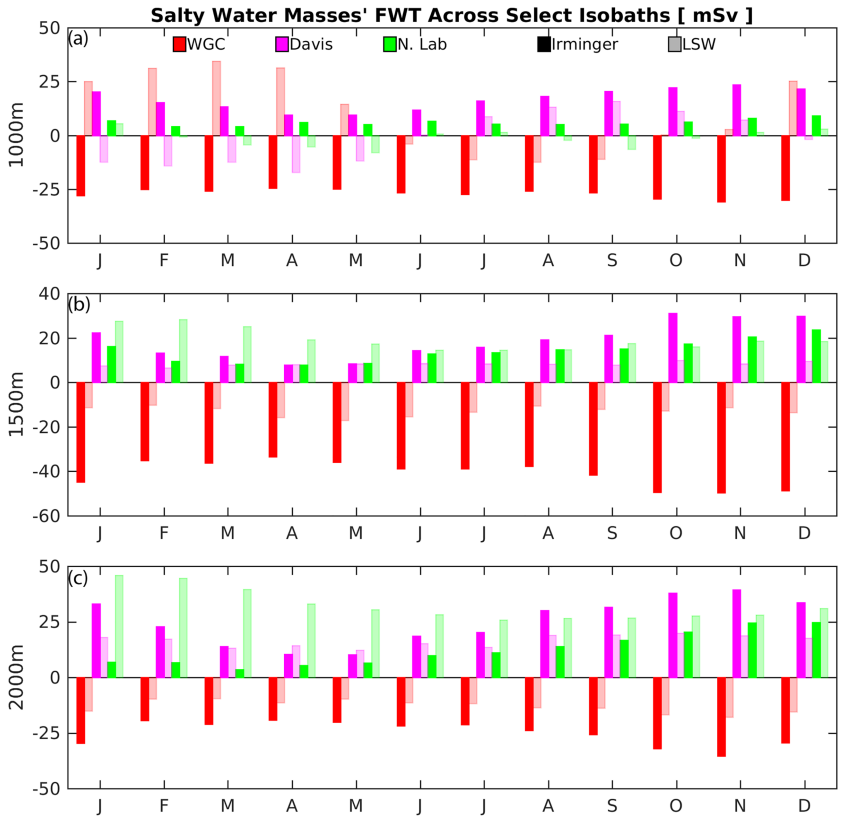

Figure 8. Monthly freshwater transport (FWT, in millisverdrup) associated with Irminger Water (opaque bars) and Labrador Sea Water (translucent) crossing three isobaths of the North Atlantic subpolar gyre: (a) 1,000 m; (b) 1,500 m; (c) 2,000 m. Three regions with significant transport are shown: red bars are for the western coast of Greenland, magenta bars for Davis Strait region, and green bars for the northern coast of Labrador. Positive values indicate an onshore import of salty water. WGC = West Greenland Coast; LSW = Labrador Sea Water.

seasonal variability and weak transport (about 5 mSv), the 1,500- and 2,000-m isobaths exhibit seasonality with a minimum in freshwater export during the late winter and early spring, and a maximum in the fall. The 2,000-m isobath also experiences a rapid decline in freshwater export between December and January which warrants further investigation.

4.4. Labrador Sea Water

Our LSW mass, defined strictly by density, shows limited seasonality across the eastern coast of Greenland, Hudson Strait, and the northern coast of Labrador (see Table 2). However, significant freshwater export occurred along the Davis Strait region (16.6 mSv) and northern Labrador coast (34.4 mSv) via onshore transport from the deep basin where LSW is produced. Illustrations and further results are provided below for regions which experienced seasonal variability or significant turbulent transport.

While the western coast of Greenland (Figure 8; translucent red bars) experienced limited seasonality across the 1,500- and 2,000-m isobaths with 10 to 18 mSv via offshore transport of saline water, transport across the 1,000-m isobath shows strong seasonality. A maximum freshwater export occurred during March (34 mSv), while a minimum occurred during the summer (−11 mSv). As there is no onshore transport across the 2,000- and 1,500-m isobaths, the changes seen across the 1,000-m isobath are not from the interior of the Labrador Sea. Rather, the seasonality across 1,000 m comes from LSW present between the 1,500- and 750-m isobaths and flows onshore as a response to circulation changes during the year. The turbulent transport of freshwater is generally very low for LSW (Table 2); however, about 20 mSv of export occurs across the 1,000-m isobath (Figure 6d). This is not only double the mean freshwater transport of the deeper isobaths but also opposite in direction. This suggests that the transport of LSW in this region is strongly driven by events with relatively short time scales, and given the water mass in question, likely tied to deep convection. However, with no

evidence of turbulent transport across isobaths deeper than 1,000 m, this signal could be related to upstream convection within the Irminger Sea which may be entrained within the East Greenland Current. A large part of this variability occurs near Fyllas Bank (see Figure 1d), where the 27.68 kg/m^3 isopycnal resides higher in the water column during the convective winter and spring (not shown) and recedes during the summer. The seasonal cycle across the 1,000-m isobath averages to a freshwater export of 10 mSv. If we consider the minimum during summer (10 mSv import) as the base transport, the seasonal cycle can be viewed as a 20-mSv onshore pulse of LSW.

The LSW mass generally has onshore transport of saline water across the Davis Strait region which manifests as a freshwater export (Figure 8; transluscent magenta bars). Similar as the above west Greenland current region, the two deepest isobaths have little seasonality, while the 1,000-m isobath shows significant changes throughout the year. While this region is close in proximately to an area which experiences cascading (Marson et al., 2017), no signal propagates across the 500- and 750-m isobaths (not shown), suggesting this seasonality is not attributed to cascading and likely a continuation of the pulse describe above. This pulse of LSW appears to return across this region, lagged 1 month from the signal present along the western coast of Greenland, with a freshwater transport which is nearly 0 mSv. Using the same process as above, the summer minimum transport is about 15 mSv. This means that about 15 mSv of the earlier pulse is returning across our Davis Strait region; most of the 20 mSv exported upstream along the western Greenland coast. The remainder of the pulse appears to cross at Hudson Strait (not shown), with little evidence of the pulse along the Labrador coast.

Significant amounts of LSW are transported onshore the northern coast of Labrador's 1,500- (15–30 mSv) and 2,000-m isobaths (26–46 mSv; translucent green bars in Figure 8). Both the 1,500- and 2,000-m isobaths show similar levels of seasonality, with a maximum in freshwater export during the winter and a minimum in summer. As this region is very close in proximity to the convection site within the Labrador Sea (Lab Sea Group, 1998), the maximum in transport across both these isobaths is indicative of recently formed LSW which has migrated toward the coast and likely entered into the Deep Western Boundary Current. This closely matches with the results of a 1/12° numerical simulation carried out by Brandt et al. (2007) who found the export of LSW to the Labrador Current was elevated from January to May. While the LSW within the Deep Western Boundary current is transported southward (Rhein et al., 2015), pathways of LSW are also east through the Charlie Gibbs Fracture Zone as well as a recirculation northward toward the interior basin (Fischer & Schott, 2002; Zantopp et al., 2017).

4.5. Impact of Resolution

The above results were derived from the ANHA12 simulation, though questions regarding the impact of horizontal resolution and the exchange of freshwater across shelf-breaks remain. Using our ANHA4 simulation, as well as an identical ANHA4 simulation with a 1/12° nest within the subpolar gyre (SPG12), we address how horizontal domain structure influences our earlier results. While each simulation is different, our sensitivity study did not allow for an understanding if the changes in freshwater transport were due to any particular setting, such as the bathymetry product used or the eddy diffusivity value. Instead, we are forced to state that differences in the simulated cross-isobath freshwater transport arise due to a variety of factors. We suspect the primary factor is higher resolution which can resolve finer-scale mesoscale processes, and we will make the assumption that all freshwater transport changes are due to horizontal resolution. However, we will indicate other sources which could promote differences between these simulations. We highlight each water mass at a single region where the ANHA12 simulation reported large freshwater transport values (sections 4.2–4.4) and compare against the ANHA4 and SPG12 simulations.

Examination of the Polar Water across the west coast of Greenland (Figures 9a and 9b) shows that the low-resolution simulation, ANHA4, exported much less freshwater across the 500-m isobath than the two 1/12° simulations, which were fairly similar. As the ANHA4 simulation resolved the boundary current here with a similar salinity as ANHA12 and SPG12 (not shown), we attribute the differences in freshwater transport to a weaker velocity field. Seasonal variability showed some disagreement across these isobaths, namely, that ANHA4 presented little variability, while ANHA12 and SPG12 had similar degrees of seasonality. The use of a nest within SPG12 resulted in a minor reduction in freshwater transport across the 500-m isobath compared against ANHA12, though the 2,000-m isobath transport was relatively similar across all three simulations. As the low-resolution simulation showed poorer performance in this region compared to both high

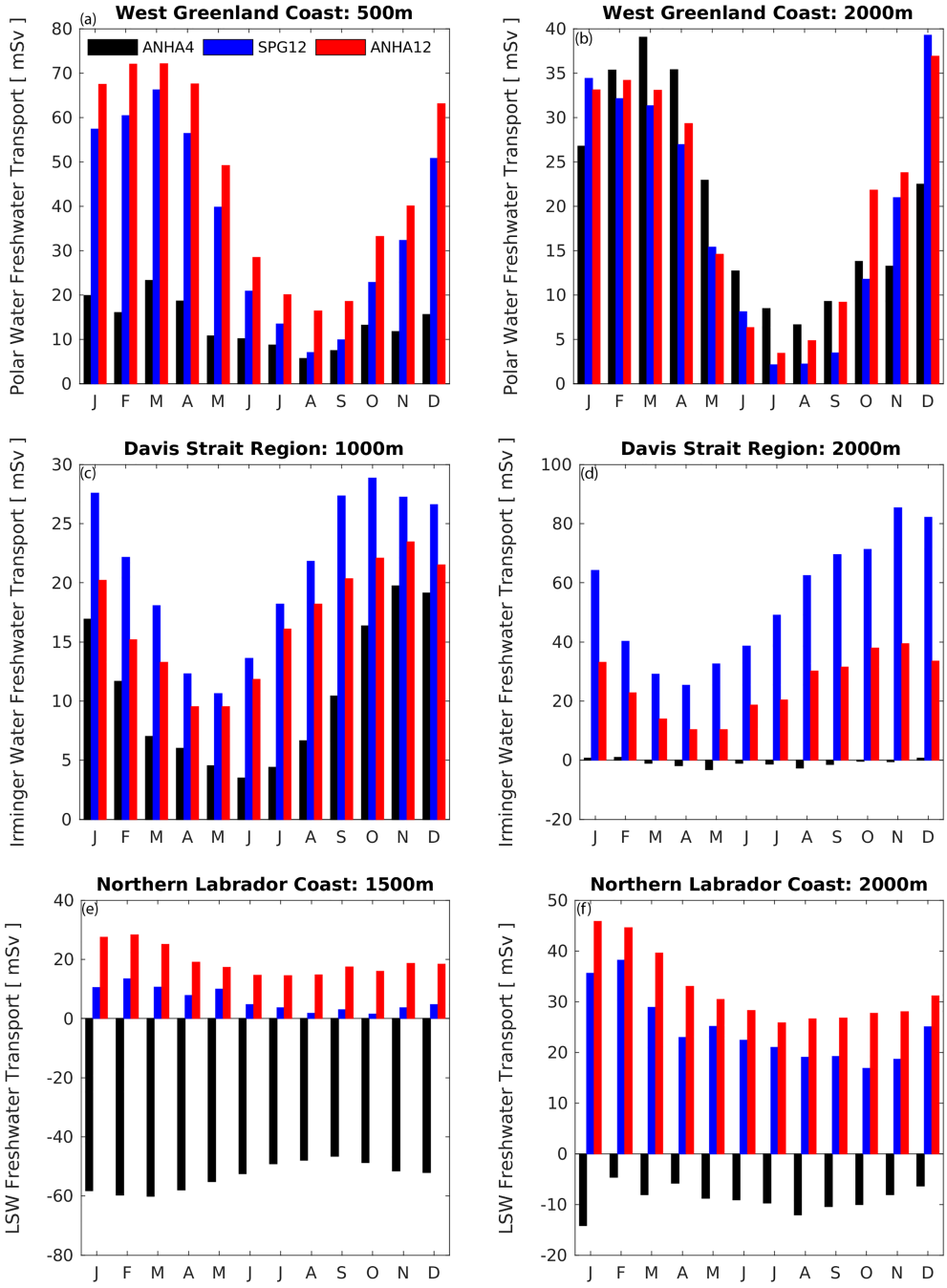

Figure 9. Monthly average freshwater transport for three different simulations: ANHA4 (black bars), SPG12 (blue) and ANHA12 (red). Three water masses are shown: Polar water crossing the (a) 500- and (b) 2,000-m isobaths of the western coast of Greenland, Irminger Water crossing the (c) 1,000- and (d) 2,000-m isobaths of the Davis Strait Region, and Labrador Sea Water crossing the (e) 1,500- and 2,000-m isobaths (f) of the Northern coast of Labrador. Positive values indicate an offshore export of freshwater or onshore import of salty water. ANHA = Arctic Northern Hemisphere Atlantic; LSW = Labrador Sea Water.

resolution simulations, this illustrates the importance of resolution in this region of high baroclinicity which promotes the development of eddies and other mesoscale features.

Irminger Water, having strong export rates across the Davis Strait region described earlier (Figure 8), showed similar seasonal variability between all simulations across the 1,000-m isobath (Figure 9c), though the

magnitude of transport was different. The transport across the 2,000-m isobath shows an interesting case where SPG12 simulated much more transport than ANHA12 while ANHA4 simulated nearly zero freshwater transport. Similar as across the western coast of Greenland described above, ANHA4 simulated less freshwater transport than the higher resolution simulations and showed noticeably reduced seasonality. While not shown, ANHA4 had a distinct lack of interannual variability while the higher resolution simulations were similar.

Large differences exist between the three simulations when examining LSW crossing the shelf break along the northern coast of Labrador (Figures 9e and 9f). The ANHA4 simulation not only had excessive freshwater transported across the 1,500-m isobath but was also opposite in direction compared against the higher resolution simulations. SPG12 was also significantly reduced compared to ANHA12, though the seasonal variability between these two simulations share similarities. ANHA4 also had low amounts of freshwater imported across the 2,000-m isobath, while the high-resolution simulations simulated larger exported transport. We suspect the ANHA4 simulation had the opposite direction of freshwater transport due to simulation of a much larger convective patch than the 1/12° simulations (not shown)

5. Discussion

Three numerical model simulations were carried out to further understand the relative freshwater and saltwater transport which occurs between the regions of the continental shelf around the western North Atlantic subpolar gyre and that of the interior basin. From the ANHA12 simulation, we note that cross-shelf freshwater transport varies across these regions. The west coast of Greenland transports a long-term (2006–2016) annual mean 21 $\pm$ 11 mSv of freshwater across the 2,000-m isobath to the interior of the Labrador Sea (Figure 5e), the only region with significant amounts of net offshore transport of freshwater with Polar Water classification. Other regions either transported freshwater onshore or transported relatively low amounts of freshwater offshore. Of this 21 mSv (Table 2), roughly two thirds was transported via the mean flow (13.3 mSv), while the remainder was from turbulent processes (7.6 mSv). While significant amounts of freshwater are exported from the western coast of Greenland, a net transport of 9 mSv is exported across the continuous 2,000-m isobath, of which −8 mSv is from mean processes and 17 mSv from turbulent processes (Table 2), suggesting the offshore transport of freshwater is dominated by short-lived features such as eddies. With minimal net offshore freshwater transport, much of the freshwater remains within the boundary current and reaches the Grand Banks, bypassing the Labrador Sea as Fratantoni and McCartney (2010) and Loder et al. (1988) also suggest.

While lateral advection of Irminger Water typically acts to restratify the Labrador Sea after convection has ceased (Cuny et al., 2002; de Jong et al., 2016), the onshore transport of this saline water also acts to freshen the Labrador Sea. About 50 mSv of saline water is transported onshore of the 2,000-m isobath across our six regions, 65 mSv of mean transport and −15 mSv from turbulent transport (Table 2). Other than the west coast of Greenland, all regions had net onshore transport of this saline water mass. While our analysis does not fully enclose the Labrador Sea, we suggest that any influence of near-coastal Irminger Water actively restratifying the Labrador Sea occurs off the western coast of Greenland; the remaining regions act to hinder restratification. This provides further elucidation of the restratification period, normally considered to include both surface freshening and subsurface heating (Straneo, 2006). However, while the net transport of salt water was onshore, the same may not occur for the net heat transport for this water mass as it is modified during its circulation around the Labrador Sea.

The cold and salty LSW acts in a similar fashion as the Irminger Water discussed above. About 42 mSv of saline water is transported onshore the continuous 2,000-m isobath of all six regions (Table 2). With very weak turbulent processes (5 mSv onshore) associated with this water mass, the mean flow (37 mSv onshore) is the primary contributor. The northern coast of Labrador, in close proximity to the Labrador Sea convection site, has the largest seasonal changes for this water mass; the 1,500- and 2,000-m isobaths have elevated onshore transport of saline water during the convective period. The west coast of Greenland, far from the convective site, also experiences an interesting seasonal pattern across the 1,000-m isobath, where a saltwater pulse of 20 mSv is onshore due to lifting of the 27.68 kg/m^3 isopycnal. This pulse passes around the northern Labrador Sea slowly leaking offshore between Davis and Hudson Strait.

Across most regions and isobaths, the transport of freshwater via turbulent flow has relatively low variability and weak transport. Some notable exceptions are Polar Water across the north and south coast of Labrador (Figure 6), both of which exhibited both strong transport and seasonality. Upstream along the west coast of Greenland, Polar Water always exported freshwater via both the mean and turbulent flow, the only region and water mass with significant transport to do so. Both the Irminger and LSW masses have limited seasonality to their turbulent processes within this region, supplying fairly constant transports across the year. These salt water masses almost always had a different direction between their mean and turbulent freshwater transport, regardless of region. While the mean and turbulent transport act opposite in directions, the magnitude of mean freshwater transport was greater than the turbulent transport (Table 2) and determines the direction of net freshwater transport per water mass. While our analysis was performed using the turbulent transport as a deviation based on a 25-day moving mean, we found that changing the averaging period to be between 10 and 35 days did not produce much difference in our results while the 25-day moving mean maximized the turbulent transport.

An increase in resolution from 1/4° to 1/12° appears to have resulted in significant changes in the cross-shelf freshwater transport within the Labrador Sea (Figure 9). At 1/4° resolution, both bathymetry and turbulent processes can be expected to be poorly resolved compared to a similar simulation with 1/12° resolution. As such, the differences in freshwater transport across certain isobaths between the ANHA4 simulation and the two 1/12° simulations were anticipated to some degree. The ANHA4 simulation not only simulated less freshwater exchange in shallow regions (<1,000 m) but also had lower seasonal variability when compared against ANHA12. We suspect the poor performance in shallow regions was in part due to poorly resolved coastal current systems. ANHA4 also suffered when simulating freshwater exchange across deeper isobaths, in some cases having nearly no net transport of Irminger Water and rather low amounts of LSW, while both 1/12° simulations showed significant transport. Perhaps most interesting was a complete directional shift between ANHA4 and the 1/12° simulations in terms of LSW; at 1,500-m depth, ANHA4 had freshwater import rates greater than the export rates of the 1/12° simulations (Figure 9e). This may be attributed to a far larger spatial extent of convection in 1/4° simulations than at 1/12° (not shown), perhaps forming LSW further onshore which is later transported offshore. This follows well with Marzocchi et al. (2015), who found a significant improvement in circulation present within the North Atlantic subpolar gyre when horizontal resolution was increased from 1/4° to 1/12°. The increase in resolution allows for an improved representation of eddies within the Labrador Sea, particularly Irminger Rings which are essential in providing heat to the interior of the Labrador Sea (Gelderloos et al., 2011), reducing the spatial extent of the convective region. Our results suggest that lower resolution not only impacts freshwater transport along the west coast of Greenland but also all water masses within the basin. These freshwater transport differences imply that low-resolution simulations will produce a Labrador Sea with a different degree of stratification than higher resolution simulations.

Fewer differences were noticed between the 1/12° simulations, though SPG12 often had additional freshwater transport compared to ANHA12. This was somewhat a surprise, due to the SPG12's domain setup, since SPG12 used nesting software to interpolate from the 1/4° parent simulation onto the 1/12° nest. We would have expected SPG12's freshwater transport values to be between that of ANHA4 and ANHA12. We attribute these differences to the nested domain's boundary conditions, which, after interpolation from the coarse parent domain, may fail to resolve the same current systems as resolved by ANHA12. As the SPG12 domain's border is rather close to Davis Strait and Hudson Strait, these are areas where boundary issues may creep into the nested domain, influencing regions downstream. While the use of nesting software allows for high resolution at a reduced computational expense, the drawbacks of nesting are not negligible.

6. Conclusions

Further clarification on the exchange of fresh and saltwater between the boundary and interior of the Labrador Sea is carried out using three numerical simulations. Liquid freshwater leaves the boundary current system and enters the deeper basin along the west coast of Greenland and the south coast of Labrador. Other regions either exchange relatively little freshwater or sequester freshwater from the interior of the Labrador Sea. However, freshwater locked within sea ice passes into deeper water across all regions, though in relatively low amounts. Salty water masses exhibit onshore transport in many regions, resulting in a freshening of the subsurface Labrador Sea. Numerical resolution appears important in resolving the

processes that drive cross-shelf freshwater transport, with significant differences between our 1/4° and 1/12° simulations. The 1/12° simulations had relatively similar cross-shelf freshwater transport despite differences in their domain construction. These results help to paint a more complete picture of the lateral exchange of fresh and saltwater between the boundary currents and the interior of the Labrador Sea by isolating particular regions where, and how much, freshwater exchange occurs. While previous studies have focused on freshwater exchange along the west Greenland coast (e.g., Myers et al., 2009; Schmidt & Send, 2007) and the Labrador coast (e.g., McGeehan & Maslowski, 2011; Myers, 2005; Schulze & Frajka-Williams, 2018), we provide estimates of the freshwater that is exchanged in other regions around the North Atlantic subpolar gyre. Furthermore, we estimate the freshwater transport via two saltwater masses and update the current knowledge on subsurface restratification within the Labrador Sea.

Climate implications of this study suggest that changes to freshwater pathways can modify the degree of stratification in the Labrador Sea. For example, Grivault et al. (2017) suggest that under a future climate scenario, the addition of freshwater and heat to Baffin Bay reduces the freshwater transport between Baffin Bay and the Labrador Sea, increasing freshwater transport around Greenland. This could cause the East and West Greenland Current systems to become fresher. With more freshwater in the West Greenland Current, a larger amount of freshwater should enter the interior of the Labrador Sea and strengthen the stratification. Furthermore, as a significant portion of meltwater from Greenland's Ice Sheet enters the Labrador Sea (Gillard et al., 2016; Luo et al., 2016), a warming climate could result with a shutdown in deep convection within the next few decades if the melting of Greenland continues at its current rate (Böning et al., 2016). On the other hand, an increase in freshwater transport to the Labrador Sea from Hudson or Baffin Bay would likely not impact the convection within the Labrador Sea as little exchange occurs downstream of these regions, as Schulze and Frajka-Williams (2018) also concluded. Although larger volumes of freshwater will be stored in the boundary currents, we do not anticipate future changes in the direction of freshwater export/import, though the magnitude of freshwater transport will likely change. This suggests that the future increased melt from Greenland that makes its way into the interior of the Labrador Sea will likely be exported from the west Greenland coast regardless of where the melt occurred. Koenigk et al. (2007) investigated that climate change simulations promoted a significant increase in freshwater export through the Canadian Archipelago, though with minimal net freshwater change through Fram Strait, somewhat at odds with Grivault et al. (2017). Our analysis suggests that the regions around the Labrador Sea export freshwater into the deep basin very differently than one another and the impact on convection depends on which region experiences any changes in freshwater.

Acknowledgments
The authors would like to express our appreciation to multiple individuals and groups. We thank the CCGS *Hudson* for data collection performed during yearly hydrographic cruises along AR7W. The altimeter products were produced by Ssalto/Duacs and distributed by Aviso, with support from Cnes (http://www.aviso.altimetry.fr/duavs/). We would like to thank Vasco Müller and Natasha Ridenour for their help producing certain figures. We would like to thank Greg Smith and Environment and Climate Change Canada for their CGRF data set used to force our simulations. We would like to thank the Compute Canada (http://www.computecanada.ca) staff for providing and maintaining the high-performance computing system which our simulations took place on. We especially would like to thank the NEMO, AGRIF, and DRAKKAR teams for the modeling software provided to perform our simulations. This work was supported by NSERC Climate Change and Atmospheric Research Grant (Grant RGPCC 433898) as well as an NSERC Discovery Grant (Grant RGPIN 04357).

References

Aagaard, K., & Carmack, E. C. (1989). The role of sea ice and other fresh water in the Arctic circulation. *Journal of Geophysical Research*, *94*(C10), 14,485–14,498. https://doi.org/10.1029/JC094iC10p14485

Amante, C., & Eakins, B. W. (2009). ETOPO1 1 Arc-minute global relief model: Procedures data sources and analysis. NOAA Technical Memorandum NESDIS, NGDC-24 19.

Avisc, T., Karstensen, J., Send, U., & Fischer, J. (2006). Interannual variability of newly formed Labrador Sea Water from 1994 to 2005. *Geophysical Research Letters*, *33*, L21S02. https://doi.org/10.1029/2006GL026913

Bacon, S., Gould, W. J., & Jia, Y. (2003). Open-ocean convection in the Irminger Sea. *Geophysical Research Letters*, *30*(5), 1246. https://doi.org/10.1029/2002GL016271

Bamber, J., van den Broeke, M., Ettema, J., Lenaerts, J., & Rignot, E. (2012). Recent large increase in freshwater fluxes from Greenland into the North Atlantic. *Geophysical Research Letters*, *39*, L19501. https://doi.org/10.1029/2012GL052552

Barnier, B., Brodeau, L., le Sommer, J.-M., Molines, T., Penduff, S., Theetten, A.-M., et al. (2007). Eddy-permitting ocean circulation hindcasts of past decades. *Clivar Exchanges*, *42*(12 (3)), 8–10.

Belkin, I. M., Levitus, S., Antonov, J., & Malmberg, S. A. (1998). "Great salinity anomalies" in the North Atlantic. *Progress in Oceanography*, *41*(1), 1–68. https://doi.org/10.1016/S0079-6611(98)00015-9

Böning, C. W., Behrens, E., Biastoch, A., Getzlaff, K., & Bamber, J. L. (2016). Emerging impact of Greenland meltwater on deepwater formation in the North Atlantic Ocean. *Nature Geoscience*, *9*(7), 523–527. https://doi.org/10.1038/ngeo2740

Brandt, P., Funk, A., Czeschel, L., Eden, C., & Böning, C. W. (2007). Ventilation and transformation of Labrador Sea Water and its rapid export in the deep Labrador Current. *Journal of Physical Oceanography*, *37*(4), 946–961. https://doi.org/10.1175/JPO3044.1

Brossier, C. L., Léger, L., Giordani, H., Beuvier, J., Bouin, M. N., Ducrocq, V., & Fourrié, N. (2017). Dense water formation in the northern-western Mediterranean area during HyMeX-SOP2 in 1/36° ocean simulations: Ocean-atmosphere coupling impact. *Journal of Geophysical Research: Oceans*, *122*, 5749–5773. https://doi.org/10.1002/2016JC012526

Chafik, L., & Rossby, T. (2019). Volume, heat, and freshwater divergences in the subpolar North Atlantic suggest the Nordic Seas as key to the state of the Meridional Overturning Circulation. *Geophysical Research Letters*, *46*, 4799–4808. https://doi.org/10.1029/2019GL082110

Chanut, J., Barnier, B., Large, W., Debreu, L., Penduff, T., Molines, J. M., & Mathiot, P. (2008). Mesoscale eddies in the Labrador Sea and their contribution to convection and restratification. *Journal of Physical Oceanography*, *28*(8), 1617–1643.

Close, S., Herbaut, C., Houssais, M. N., & Blaizot, A. C. (2018). Mechanisms of interannual-to decadal-scale winter Labrador Sea ice variability. *Climate Dynamics*, *51*(7-8), 2485–2508. https://doi.org/10.1007/s00382-017-4024-z

Courtois, P., Hu, X., Pennelly, C., Spence, P., & Myers, P. G. (2017). Mixed layer depth calculation in deep convection regions in ocean numerical models. *Ocean Modelling*, *120*, 60–78. https://doi.org/10.1016/j.ocemod.2017.10.007

Cuny, J., Rhines, P. B., & Kwok, R. (2005). Davis Strait volume, freshwater and heat fluxes. *Deep Sea Research Part I: Oceanographic Research Papers*, *52*(3), 519–542. https://doi.org/10.1016/j.dsr.2004.10.006

Cuny, J., Rhines, P. B., Niiler, P. P., & Bacon, S. (2002). Labrador Sea boundary currents and the fate of the Irminger Sea Water. *Journal of Physical Oceanography*, *32*(2), 627–647. https://doi.org/10.1175/1520-0485(2002)032<0627:LSBCAT>2.0.CO;2

Curry, B., Lee, C. M., Petrie, B., Moritz, R. E., & Kwok, R. (2014). Multiyear volume, liquid freshwater, and sea ice transports through Davis Strait, 2004–10. *Journal of Physical Oceanography*, *44*(4), 1244–1266. https://doi.org/10.1175/JPO-D-13-0177.1

Curry, B. C., Lee, C. M., & Petrie, B. (2011). Volume, freshwater, and heat fluxes through Davis Strait, 2004–2005. *Journal of Physical Oceanography*, *41*(3), 429–436. https://doi.org/10.1175/2010JPO4536.1

Dai, A., Qian, T., Trenberth, K. E., & Milliman, J. D. (2009). Changes in continental freshwater discharge from 1948 to 2004. *Journal of Climate*, *22*(10), 2773–2792. https://doi.org/10.1175/2008JCLI2592.1

de Jong, M. F., Bower, A. S., & Furey, H. H. (2016). Seasonal and interannual variations of Irminger ring formation and boundary-interior heat exchange in FLAME. *Journal of Physical Oceanography*, *46*(6), 1717–1734. https://doi.org/10.1175/JPO-D-15-0124.1

de Steur, L., Hansen, E., Gerdes, R., Karcher, M., Fahrbach, E., & Holfort, J. (2009). Freshwater fluxes in the East Greenland Current: A decade of observations. *Geophysical Research Letters*, *36*, L23611. https://doi.org/10.1029/2009GL041278

de Steur, L., Peralta-Ferriz, C., & Pavlova, O. (2018). Freshwater export in the East Greenland Current freshens the Northern Atlantic. *Geophysical Research Letters*, *45*, 13,359–13,366. https://doi.org/10.1029/2018GL080207

de Steur, L., Pickart, R. S., Macrander, A., Våge, K., Harden, B., Jónsson, S., et al. (2017). Liquid freshwater transport estimates from the East Greenland Current based on continuous measurements north of Denmark Strait. *Journal of Geophysical Research: Oceans*, *122*, 93–109. https://doi.org/10.1002/2016JC012106

Debreu, L., Vouland, C., & Blayo, E. (2008). AGRIF: Adaptive grid refinement in Fortran. *Computers and Geosciences*, *34*(1), 8–13. https://doi.org/10.1016/j.cageo.2007.01.009

Dickson, R. R., Meincke, J., Malmberg, S. A., & Lee, A. J. (1988). The great salinity anomaly: In the northern North Atlantic 1968–1982. *Progress in Oceanography*, *20*(2), 103–151. https://doi.org/10.1016/0079-6611(88)90049-3

Ferry, N., Parent, L., Garric, G., Barnier, B., & Jourdain, N. C. (2010). Mercator global eddy permitting ocean reanalysis GLORYS1V1: Description and results. *Mercator-Ocean Quarterly Newsletter*, *36*, 15–27.

Feucher, C. E., Garcia-Quintana, Y., Yashayaev, I., Hu, X., & Myers, P. G. (2019). Labrador Sea Water formation rate and its impact on the local Meridional Overturning Circulation. *Journal of Geophysical Research: Oceans*. *124*, 5654–5670. https://doi.org/10.1029/2019JC015065

Fichefet, T., & Maqueda, M. A. M. (1997). Sensitivity of a global sea ice model to the treatment of ice thermodynamics and dynamics. *Journal of Geophysical Research*, *102*(C6), 12,609–12,646. https://doi.org/10.1029/97JC00480

Fischer, J., & Schott, F. A. (2002). Labrador Sea Water tracked by profiling floats—From the boundary current into the open North Atlantic. *Journal of Physical Oceanography*, *32*(2), 573–584. https://doi.org/10.1175/1520-0485(2002)032<0573:LSWTBP>2.0.CO;2

Fischer, J., Visbek, M., Zantopp, R., & Nunes, N. (2010). Interannual to decadal variability of outflow from the Labrador Sea. *Geophysical Research Letters*, *37*, L24610. https://doi.org/10.1029/2010GL045321

Frajka-Williams, E., Rhines, P. B., & Eriksen, C. C. (2014). Horizontal stratification during deep convection in the Labrador Sea. *Journal of Physical Oceanography*, *44*(1), 220–228. https://doi.org/10.1175/JPO-D-13-069.1

Fratantoni, P. S., & McCartney, M. S. (2010). Freshwater export from the Labrador Current to the North Atlantic Current and the tail of the Grand Banks of Newfoundland. *Deep Sea Research Part I: Oceanographic Research Papers*, *57*(2), 258–283. https://doi.org/10.1016/j.dsr.2009.11.006

Gelderloos, R., Katsman, C. A., & Drijfhout, S. S. (2011). Assessing the roles of three eddy types in restratifying the Labrador Sea after deep convection. *Journal of Physical Oceanography*, *4*(11), 2102–2119.

Gelderloos, R., Straneo, F., & Katsman, C. A. (2012). Mechanisms behind the temporary shutdown of deep convection in the Labrador Sea: Lessons from the great salinity anomaly years 1968–71. *Journal of Climate*, *25*(19), 6743–6755. https://doi.org/10.1175/JCLI-D-11-00549.1

Gillard, L., Hu, X., Myers, P. G., & Bamber, J. L. (2016). Meltwater pathways from marine terminating glaciers of the Greenland ice sheet. *Geophysical Research Letters*, *43*, 10,873–10,882. https://doi.org/10.1002/2016GL070969

Gordon, A. L., Visbeck, M., & Comiso, J. C. (2007). A possible link between the Weddell Polynya and the Southern Annular Mode. *Journal of Climate*, *20*(11), 2558–2571. https://doi.org/10.1175/JCLI4046.1

Grivault, N., Hu, X., & Myers, P. G. (2017). Evolution of Baffin Bay water masses and transports in a numerical sensitivity experiment under enhanced Greenland Melt. *Atmosphere-Ocean*, *55*(3), 169–194. https://doi.org/10.1080/07055900.2017.1333950

Grivault, N., Hu, X., & Myers, P. G. (2018). Impact of the surface stress on the volume and freshwater transport through the Canadian Arctic Archipelago from high resolution numerical modelling. *Journal of Geophysical Research: Oceans*, *123*, 9038–9060. https://doi.org/10.1029/2018JC013984

Häkkinen, S., & Rhines, P. B. (2004). Decline of subpolar North Atlantic circulation during the 1990s. *Science*, *304*(5670), 555–559. https://doi.org/10.1126/science.1094917

Handmann, P., Fischer, J., Visbeck, M., Karstensen, J., Biastoch, A., Böning, C., & Patara, L. (2018). The deep western boundary current in the Labrador Sea from observations and a high-resolution model. *Journal of Geophysical Research: Oceans*, *123*, 2828–2850. https://doi.org/10.1002/2017JC013702

Hansen, B., & Østerhus, S. (2000). North Atlantic-Nordic Seas exchanges. *Progress in Oceanography*, *45*(2), 109–208. https://doi.org/10.1016/S0079-6611(99)00052-X

Holdsworth, A. M., & Myers, P. G. (2015). The influence of high-frequency atmospheric forcing on the circulation and deep convection of the Labrador Sea. *Journal of Climate*, *28*(12), 4980–4996. https://doi.org/10.1175/JCLI-D-14-00564.1

Howatt, T., Palter, J. B., Matthews, R., deYoung, B., Bachmayer, R., & Claus, R. (2018). Ekman and eddy exchange of freshwater and oxygen across the Labrador shelf break. *Journal of Physical Oceanography*, *48*(5), 1015–1031. https://doi.org/10.1175/JPO-D-17-0148.1

Hu, X., Sun, J., Chan, T. O., & Myers, P. G. (2018). Thermodynamic and dynamic ice thickness contributions in the Canadian Arctic Archipelago in NEMO-LIM2 numerical simulations. *The Cryosphere*, *12*(4), 1233–1247. https://doi.org/10.5194/tc-12-1233-2018

Hughes, K. G., Klymak, J. M., Hu, X., & Myers, P. G. (2017). Water mass modification and mixing rates in a 1/12° simulation of the Canadian Arctic Archipelago. *Journal of Geophysical Research: Oceans*, *122*, 803–820. https://doi.org/10.1002/2016JC012235

Jia, F., Wu, L., Lan, J., & Qiu, B. (2011). Interannual modulation of eddy kinetic energy in the southeast Indian Ocean by Southern Annular Mode. *Journal of Geophysical Research*, *116*, C02029. https://doi.org/10.1029/2010JC006699

Jonsson, S., & Valdimarsson, H. (2004). A new path for the Denmark Strait overflow water from the Iceland Sea to Denmark Strait. *Geophysical Research Letters*, *31*, L03305. https://doi.org/10.1029/2003GL019214

Kawasaki, T., & Hasumi, H. (2014). Effect of freshwater from the West Greenland Current on the winter deep convection in the Labrador Sea. *Ocean Modelling*, *75*, 51–64. https://doi.org/10.1016/j.ocemod.2014.01.003

Khatiwala, S., Schlosser, P., & Visbeck, M. (2002). Rates and mechanisms of water mass transformation in the Labrador Sea as inferred from tracer observations. *Journal of Physical Oceanography*, *32*(2), 666–686. https://doi.org/10.1175/1520-0485(2002)032<0666:RAMOWM>2.0.CO;2

Kieke, D., Rhein, M., Stramma, L., Smethie, W. M., LeBel, D. A., & Zenk, W. (2006). Changes in the CFC inventories and formation rates of Upper Labrador Sea Water, 1997-2001. *Journal of Physical Oceanography*, *36*(1), 64–86. https://doi.org/10.1175/JPO2814.1

Koenigk, T., Mikolajewicz, U., Haak, U., & Jungclaus, J. (2007). Arctic freshwater export in the 20th and 21st centuries. *Journal of Geophysical Research*, *112*, G04S41. https://doi.org/10.1029/2006JG000274

Lab Sea Group (1998). The Labrador Sea deep convection experiment. *Bulletin of the American Meteorological Society*, *79*(10), 2033–2058. https://doi.org/10.1175/1520-0477(1998)079<2033:TLSDCE>2.0.CO;2

Lazier, J., Hendry, R., Clarke, A., Yashayaev, I., & Rhines, P. (2002). Convection and restratification in the Labrador Sea, 1990–2000. *Deep Sea Research Part I: Oceanographic Research Papers*, *49*(10), 1819–1835. https://doi.org/10.1016/S0967-0637(02)00064-X

Lazier, J. R. (1980). Oceanographic conditions at ocean weather ship Bravo, 1964–1974. *Atmosphere-Ocean*, *18*(3), 227–238. https://doi.org/10.1080/07055900.1980.9649089

Lazier, J. R. N., & Wright, D. G. (1993). Annual velocity variations in the Labrador Current. *Journal of Physical Oceanography*, *23*(4), 659–678. https://doi.org/10.1175/1520-0485(1993)023<0659:AVVITL>2.0.CO;2

Lilly, J. M., Rhines, P. B., Visbeck, M., Davis, R., Lazier, J. R. N., Schott, F., & Farmer, D. (1999). Observing deep convection in the Labrador Sea during winter 1994/95. *Journal of Physical Oceaongraphy*, *29*(8), 2065–2098. https://doi.org/10.1175/1520-0485(1999)029<2065:ODCITL>2.0.CO;2

Lin, P., Pickart, R. S., Torres, D. J., & Pacini, A. (2018). Evolution of the freshwater coastal current at the southern tip of Greenland. *Journal of Physical Oceanography*, *48*(9), 2127–2140. https://doi.org/10.1175/JPO-D-18-0035.1

Loder, J. W., Ross, C. K., & Smith, P. C. (1988). A space-and time-scale characterization of circulation and mixing over submarine banks, with application to the northwestern Atlantic continental shelf. *Canadian Journal of Fisheries and Aquatic Sciences*, *45*(11), 1860–1885. https://doi.org/10.1139/f88-219

Lozier, M. S., Li, F., Bacon, S., Bahr, F., Bower, A. S., Cunningham, S. A., et al. (2019). A sea change in our view of overturning in the subpolar North Atlantic. *Science*, *363*(6426), 516–521. https://doi.org/10.1126/science.aau6592

Luo, H., Bracco, A., & Di Lorenzo, E. (2011). The interannual variability of the surface eddy kinetic energy in the Labrador Sea. *Progress in Oceanography*, *91*(3), 295–311. https://doi.org/10.1016/j.pocean.2011.01.006

Luo, H., Castelao, R. M., Rennermalm, A. K., Tedesco, M., Bracco, A., Yager, P. L., & Mote, T. L. (2016). Oceanic transport of surface meltwater from the southern Greenland ice sheet. *Nature Geoscience*, *9*(7), 528–532. https://doi.org/10.1038/ngeo2708

Madec, G. (2008). Note du Pôle de modélisation, Institut Pierre-Simon Laplace (IPSL), France, No 27, ISSN No 1288-1619.

Marshall, J., & Schott, F. (1999). Open-ocean convection: Observations, theory, and models. *Reviews of Geophysics*, *37*(1), 1–64. https://doi.org/10.1029/98RG02739

Marson, J. M., Myers, P. G., Hu, X., Petrie, B., Azetsu-Scott, K., & Lee, C. M. (2017). Cascading off the West Greenland shelf: A numerical perspective. *Journal of Geophysical Research: Oceans*, *122*, 5316–5328. https://doi.org/10.1002/2017JC012801

Marzocchi, A., Hurschi, J. J. M., Holliday, N. P., Cunningham, S. A., Blaker, A. T., & Coward, A. C. (2015). The North Atlantic subpolar circulation in an eddy-resolving global ocean model. *Journal of Marine Systems*, *142*, 126–143. https://doi.org/10.1016/j.jmarsys.2014.10.007

McGeehan, I., & Maslowski, W. (2011). Impact of shelf-basin freshwater transport on deep convection in the western Labrador Sea. *Journal of Physical Oceanography*, *41*(11), 2187–2210. https://doi.org/10.1175/JPO-D-11-01.1

Müller, V., Kieke, D., Myers, P. G., Pennelly, C., & Mertens, C. (2017). Temperature flux carried by individual eddies across 47° N in the Atlantic Ocean. *Journal of Geophysical Research: Oceans*, *122*, 2441–2464. https://doi.org/10.1002/2016JC012175

Müller, V., Kieke, D., Myers, P. G., Pennelly, C., Steinfeldt, R., & Stendardo, I. (2019). Heat and freshwater transport by mesoscale eddies in the southern subpolar North Atlantic. *Journal of Geophysical Research: Oceans*, *124*, 5565–5585. https://doi.org/10.1029/2018JC014697

Myers, P. (2005). Impact of freshwater from the Canadian Arctic Archipelago on the Labrador Sea water formation. *Geophysical Research Letters*, *32*, L06605. https://doi.org/10.1029/2004GL022082

Myers, P. G., Donnelly, C., & Ribergaard, M. H. (2009). Structure and variability of the West Greenland Current in summer derived from 6 repeat standard sections. *Progress in Oceanography*, *80*(1-2), 93–112. https://doi.org/10.1016/j.pocean.2008.12.003

Myers, P. G., Kulan, N., & Ribergaard, M. H. (2007). Irminger water variability in the West Greenland Current. *Geophysical Research Letters*, *34*, L17601. https://doi.org/10.1029/2007GL030419

Fratantoni, P. S., & Pickart, R. S. (2007). The western North Atlantic shelfbreak current system in summer. *Journal of Physical Oceanography*, *37*(10), 2509–2533.

Pickart, R. S., & Spall, M. A. (2007). Impact of Labrador Sea convection on the North Atlantic meridional overturning circulation. *Journal of Physical Oceanography*, *37*(9), 2207–2227. https://doi.org/10.1175/JPO3178.1

Quartly, G. D., de Cuevas, B. A., & Coward, A. C. (2013). Mozambique Channel eddies in GCMs: A question of resolution and slippage. *Ocean Modelling*, *63*, 56–67. https://doi.org/10.1016/j.ocemod.2012.12.011

Rattan, S., Myers, P. G., Treguier, A. M., Theetten, S., Biastoch, A., & Böning, C. (2010). Towards and understanding of Labrador Sea salinity drift in eddy-permitting simulations. *Ocean Modelling*, *35*(1-2), 77–88. https://doi.org/10.1016/j.ocemod.2010.06.007

Rhein, N., Kieke, D., & Steinfeldt, R. (2015). Advection of North Atlantic Deep Water from the Labrador Sea to the Southern Hemisphere. *Journal of Geophysical Research: Oceans*, *120*, 2471–2487. https://doi.org/10.1002/2014JC010605

Rieck, J. K., Böning, C. W., & Getzlaff, K. (2019). The nature of eddy kinetic energy in the Labrador Sea: Different types of mesoscale eddies, their temporal variability and impact on deep convection. *Journal of Physical Oceanography*, *49*(8), 2075–2094. https://doi.org/10.1175/JPO-D-18-0243.1

Rykova, T., Straneo, F., & Bower, A. S. (2015). Seasonal and interannual variability of the West Greenland Current System in the Labrador Sea in 1993–2008. *Journal of Geophysical Research: Oceans*, *120*, 1318–1332. https://doi.org/10.1002/2014JC010386

Saenko, O. A., Dupont, F., Yang, D., Myers, P. G., Yashayaev, I., & Smith, G. C. (2014). Role of resolved and parameterized eddies in the Labrador Sea balance of heat and buoyancy. *Journal of Physical Oceanography*, *44*(12), 3008–3032. https://doi.org/10.1175/JPO-D-14-0041.1

Schmidt, S., & Send, U. (2007). Origin and composition of seasonal Labrador Sea freshwater. *Journal of Physical Oceanography*, *37*(6), 1445–1454. https://doi.org/10.1175/JPO3065.1

Schulze, C. L. M., & Frajka-Williams, E. (2018). Wind-driven transport of fresh shelf water into the upper 30 m of the Labrador Sea. *Ocean Science*, *14*(5), 1247–1264. https://doi.org/10.5194/os-14-1247-2018

Smith, G. C., Roy, F., Mann, P., Dupont, F., Brasnett, B., Lemieux, J. F., et al. (2014). A new atmospheric dataset for forcing ice-ocean models: Evaluation of reforecasts using the Canadian global deterministic prediction system. *Quarterly Journal of the Royal Meteorological Society*, *140*(680), 881–894. https://doi.org/10.1002/qj.2194

Smith, W. H. F., & Sandwell, D. T. (1997). Global seafloor topography from satellite altimetry and ship depth soundings. *Science*, *277*, 1957–1962.

Straneo, F. (2006). Heat and freshwater transport through the central Labrador Sea. *Journal of Physical Oceanography*, *36*(4), 606–628. https://doi.org/10.1175/JPO2875.1

Straneo, F., & Saucier, F. (2008a). *The arctic-subarctic exchange through Hudson Strait. Arctic-Subarctic Ocean Fluxes* (pp. 249–261). Dordrecht: Springer.

Straneo, F., & Saucier, F. (2008b). The outflow from Hudson Strait and its contribution to the Labrador Current. *Deep Sea Research Part I: Oceanographic Research Papers*, *55*(8), 926–946. https://doi.org/10.1016/j.dsr.2008.03.012

Sutherland, D. A., & Pickart, R. S. (2008). The East Greenland coastal current: Structure, variability, and forcing. *Progress in Oceanography*, *78*(1), 58–77. https://doi.org/10.1016/j.pocean.2007.09.006

Swift, J. H. (1984). The circulation of the Denmark Strait and Iceland-Scotland overflow waters in the North Atlantic. *Deep Sea Research Part A. Oceanographic Research Papers*, *31*(11), 1339–1355. https://doi.org/10.1016/0198-0149(84)90005-0

Tréquier, A. M., Theetten, S., Chassignet, E. P., Penduff, T., Smith, R., Talley, L., et al. (2005). The North Atlantic subpolar gyre in four high-resolution models. *Journal of Physical Oceanography*, *35*(5), 757–774. https://doi.org/10.1175/JPO2720.1

Tsubouchi, T., Bacon, S., Naveira Garabato, A. C., Aksenov, Y., Laxon, S. W., Fahrbach, E., et al. (2012). The Arctic Ocean in summer: A quasi-synoptic inverse estimate of boundary fluxes and water mass transformation. *Journal of Geophysical Research*, *117*, C01024. https://doi.org/10.1029/2011JC007174

Volkov, D. L., Larnicol, G., & Dorandeu, J. (2007). Improving the quality of satellite altimetry data over continental shelves. *Journal of Geophysical Research*, *112*, C06020. https://doi.org/10.1029/2006JC003765

Whiteworth, T., & Orsi, A. H. (2006). Antarctic Bottom Water production and export by tides in the Ross Sea. *Geophysical Research Letters*, *33*, L12609. https://doi.org/10.1029/2006GL026357

Yashayaev, I. (2007). Hydrographic changes in the Labrador Sea, 1960–2005. *Progress in Oceanography*, *73*(3-4), 242–276. https://doi.org/10.1016/j.pocean.2007.04.015

Yashayaev, I., & Loder, J. W. (2009). Enhanced production of Labrador Sea water in 2008. *Geophysical Research Letters*, *36*, L01606. https://doi.org/10.1029/2008GL036162

Yashayaev, I., & Loder, J. W. (2017). Further intensification of deep convection in the Labrador Sea in 2016. *Geophysical Research Letters*, *44*, 1429–1438. https://doi.org/10.1002/2016GL071668

Zalesak, S. T. (1979). Fully multidimensional flux-corrected transport algorithms for fluids. *Journal of Computational Physics*, *31*(3), 335–362. https://doi.org/10.1016/0021-9991(79)90051-2

Zantopp, R., Fischer, J., Visbek, M., & Karstensen, J. (2017). From interannual to decadal: 17 years of boundary current transports at the exit of the Labrador Sea. *Journal of Geophysical Research: Oceans*, *122*, 1724–1748. https://doi.org/10.1002/2016JC012271